The Pennsylvania State University

The Graduate School

Department of Civil and Environmental Engineering

A NONSTATIONARY UNCERTAINTY FRAMEWORK FOR CLIMATE CHANGE IMPACT PROJECTIONS – TRADING SPACE-FOR-TIME TO UNDERSTAND STREAMFLOW ELASTICITY

A Thesis in

Civil Engineering

by

Riddhi Singh

Submitted in Partial Fulfillment
of the Requirements
for the Degree of

Master of Science

December 2010

The thesis of Riddhi Singh was reviewed and approved* by the following:

Thorsten Wagener
Associate Professor of Civil and Environmental Engineering
Thesis Advisor

Patrick Reed
Associate Professor of Civil and Environmental Engineering

Christopher Duffy
Professor of Civil and Environmental Engineering

Peggy Johnson
Professor of Civil and Environmental Engineering
Head of the Department of Department

*Signatures are on file in the Graduate School

ABSTRACT

Watershed models are used to simulate the streamflow for a given climatic scenarios and also for ungauged basins. They have become increasingly important to predict the behavior of watersheds under the expected climate change where the watersheds will experience climates which will be much different from their historical climate. Most of the waterheds models require a simulation based approach to arrive at optimal parameter sets. One of the major problems is dependence of watershed models on calibration, whose outcome is dependent on the climatic regime of the calibration data, or on a priori parameter estimates, which often perform poorly even in reproducing historical data. In addition there is an urgent need to for the estimation of uncertainty in climate change impact assessment.

Streamflow elasticity is defined as the percent change in streamflow for a percent change in precipitation or temperature. It is an indicator of the sensitivity of streamflow to climate change. Elasticity can be derived from historical observations or from watershed model simulations.

In this study we develop a new uncertainty framework utilizing trading-space-for-time to establish model constraints that reduce predictive uncertainty while accounting for the impact of climate nonstationarity on parameter estimates. The driving hypothesis is that observed spatial gradients in watershed signatures such as runoff ratio, baseflow index etc can be used as a proxy for temporal gradients. Thus, relationships developed over vast spatial extent spanning a variety of watersheds and climate, can be used to predict the nature of a watershed as it moves to climates that it never experienced before.

The main conclusion of the study is that as we move towards more extreme climates, the importance of including nonstationarity in parameters increases. Moreover, drier climates are more sensitive to climate change than wetter climates for most of the watersheds considered in the study. The latter scenario is likely to be the case for many less developed countries, which typically already lie in regions where water availability is lower and climate variability is higher. The results shown here suggest that previously used frameworks will likely underestimate the hydrologically-controled risks posed by climate change!

TABLE OF CONTENTS

LIST OF FIGURES

LIST OF TABLES

ACKNOWLEDGEMENTS

I express my gratitude towards Dr. Thorsten Wagener, whose constant guidance enabled me to understand the pulse of the problems that hydrology faces today. His positive and inquisitive attitude towards science inspired me to look at difficult problems with patience and understanding. I would like to thank the other members of my committee, Dr. Patrick Reed, Dr. Christopher Duffy and Dr. Peggy Johnson for the comments and discussions this work. I would also like to thank Dr. Katie VanWekhoven without whom this thesis would not be possible.

I would like to give special thanks to Keith Sawicz and Christa Keller who provided me with advice on various technical issues that came up. The time they spent with me and their advice has been indispensable.

I also thank Tom Votlz, Susan Gregg, Joseph Kasprzyk, Joshua Kollat, Adam Ward, George Holmes III, Xuan Hu and many other friends for providing me with support throughout my research work. Their presence provided a lively and encouraging atmosphere.

In the end, I would like to thank my family for supporting my vision to pursue my career at a foreign university, far from them. Without their consent, none of this would be possible.

Partial support for the first and second authors of this work has been provided by the US Department of Energy. Support for the third author was provided by the Henry Luce Foundation in the form of a Clare Booth Luce Fellowship, and by the Pennsylvania State University through College of Engineering and GE Faculty for the Future Fellowships.

Dedication

To my parents, Ved and Neeta, and to my brothers, Abhishek and Shaswat

Chapter 1

Introduction

Global problem of understanding climate change impacts

Global climate change is posing a challenge to hydrological science. Since its impacts are likely to alter freshwater resources availability in many regions of the world, there is therefore an urgent need to understand how climate change will propagate into regional hydrology, i.e. the scale of decision-making [*Wagener et al.*, 2010]. To manage water resources in the context of high hydrologic variability, potentially changes in mean flows and an increasing occurrence of extremes, we are interested in predicting the response of environmental systems with respect to any hydrologically-controlled endpoints relevant for the management of water resources or to understand aquatic ecosystem health and biodiversity. For developing management strategies for water resources we need credible tools to make such projections at relevant scales including estimates of uncertainty for effective risk assessment and adaptation.

To aid the management strategies we need characterization tools to assess the extremity of expected impact. One measure to quantify the sensitivity of hydrological systems to climate change is streamflow elasticity. In one of the first studies of its kind, *Schaake and Nemek* (1982) forced a hydrologic model calibrated on historical period with a changed precipitation and temperature forcing to estimate runoff sensitivity and concluded that sensitivity is higher for arid areas as compared to humid. Several studies followed which attempted to give a theoretical definition to elasticity and applying them to outputs from a hydrologic model to evaluate elasticity values for given watersheds. *Schaake and Liu* (1989) developed a map of streamflow elasticity due to precipitation change for the United States in

such a manner. Other studies that also derived predictions of elasticity using hydrologic models include *Nash and Gleick* [1990], *Jones et al.*[2006] and *Fu et al.*[2007]. These studies include both numerical estimates of elasticity and contour maps developed across a range of climate change regimes. The studies by *Dooge* [1992] and *Dooge et al.* [1999] focused on analytical methods of obtaining elasticity as a function of climate. Some studies like *Vogel et al.*[1999] evaluate elasticity based on regression models. *Risbey and Entekhabi* [1996] developed contour plots of elasticity for the Sacremento river basin by using data records of 100 years. They computed elasticity directly from historical records. An extensive study on the different definitions of elasticity and their applicability has been carried out by *Sankarasubramanian et al.* [2001]. They compared various methods of obtaining elasticity. One of their important conclusions is that elasticity is a model dependent quantity. They showed that estimates of precipitation elasticity depends on both model choice and model calibration by evaluating elasticity by different models. Elasticity, in general, is computed from output derived from hydrologic model or from observed records. The basic definition is given by *Schaake and Liu* [1989] :

$$\frac{\delta Q}{Q} = \Phi \frac{\delta X}{X} \qquad (1)$$

Where, Q is the historical mean flow and δQ is the departure from this historical value due; X can be precipitation or evapotranspiration; δX is the departure from the historical value of X. Therefore Φ can be precipitation elasticity or evapotranspiration elasticity of streamflow. It is to be noted that this definition is general and can be applied to both simulated and observed runoff. However, recent methods to obtain the value of elasticity focus on forcing a hydrologic model calibrated on historical regime with changed inputs as expected from climate change since it allows for an assessment of a wider climatic range. In this paper, we focus on the derivation of elasticity from simulated streamflow.

Approaches used until now and their drawbacks

But also outside the goal of obtaining elasticity estimates, we ultimately depend on the use of watershed models to achieve continuous streamflow predictions since statistical approaches will not allow us to extrapolate under nonstationary conditions [*Milly et al.*, 2008]. Many studies have used watershed scale models for climate change impact assessment [*Zheng et al.*, 2009; *Jha et al.*, 2004; *Legesse et al.*, 2010; *Knowles*, 2002, *Chiew et al.*, 2009]. The general approach adopted in these studies is to force a watershed model with downscaled climate change projections of precipitation and temperature. Most do not yet include a feedback from the hydrological model to the atmosphere. Current limitations of this approach, among other things, include in many cases a lack of consideration of uncertainty and of the nonstationarity in the parameters of the hydrological model as well. This non stationarity has been observed in several studies and has been discussed in detail in the subsequent text.The need for the inclusion of uncertainties in these projections has been motivated elsewhere and will not be repeated here [e.g. *Buytaert et al.*, 2009; *Maurer et al.*, 2005; *Ghosh et al.*, 2009]. These studies have focused on the impact of input data uncertainty arising from the use of different GCM models and downscaling techniques. However, uncertainties also stem from nonuniqueness of parameters and from errors in hydrologic model structures. The study by *Wilby et al.* [2006] attempted at incorporating hydrologic model uncertainty along with GCM uncertainties in a probabilistic framework. They found that uncertainty in the streamflow prediction due to uncertainty in hydrologic model parameters was significant and could not be neglected. However, they only attempt to quantify this uncertainty, we still need to find a method to assess the impact of changing climate on model parameters. It is expected that climate change impact projections will be even more uncertain than simulations driven by historical observations which makes it unlikely that deterministic change impact projections will be very robust and a good basis for risk assessment or decision-making. Although

different sources of uncertainty will affect such impact projections; here we will focus on the uncertainty introduced through the model parameters under nonstationary conditions.

Parameters in watershed models are generally derived via two strategies: calibration on historical observations or through a priori parameter estimation.

- A priori estimates of parameters are derived by relating model parameters to physical characteristics of the watershed such as soil, vegetation etc. However, studies have shown that a priori parameter estimates have a high degree of uncertainty attached to them, lack robustness and can often produce low performance [*Duan et.al,* 2006; *van Werkhoven et al.* 2009*; Hughes and Kapangaziwiri,* 2009]. Hence, model calibration has generally been found to produce more reliable estimates of parameters.
- During calibration, the parameter set that produces the best fit between simulated and observed streamflow is identified. Different strategies have been developed to consider the uncertainty in this identification process when historical observations are used or when the model is applied to ungauged watersheds [*Clark and Vrugt,* 2006*; Khadam and Kaluarachchi,* 2004].

More recently it has been observed that the climatic regime of the time period in which the calibration data have been observed leaves an imprint in the parameter estimates [e.g. *Van Werkhoven et al.,* 2008*; Vaze et al.,* 2009]. A recent study by *Merz et. al* [2010] for example analyzes how calibrated parameters might change with climate. They found that the parameters used for their model showed clear time trends when calibrated on different periods. In other words, parameters were found to be function climate regime of the period of calibration. They suggest that explicitly accounting for non-stationary model parameters is one of the potential solutions for assessing climate change impact on streamflows. This implies that the parameter set obtained by calibrating over a wet period can be different than what we obtain by calibrating over a dry period and vice versa. This has potential implications for climate change impact studies where the climate is by definition different

from historical observations. *Vaze et al.* [2009] carried out a study to examine the validity of using historically calibrated rainfall runoff models for future climate change predictions. Their modeling study quantifies the departure from mean rainfall after which the applicability of historical model parameters becomes unsuitable for the new climate regime. Again, they point out to the problem of nonstationarity of parameters but we still need to identify a methodology to deal with this. *Van Werkhoven et al.* [2008] also point out that calibrated parameters depend on the period of record used for calibration and that the sensitivity of the parameters varies with climate. Hence, the functional behavior of the model also varies. We therefore hypothesize that a nonstationary uncertainty framework is needed to account for the required change of watershed model parameters in a changing climate.

The observed nonstationarity can be caused either by a change in the processes occurring in the watershed or by a change in the parameters of the model. In order to distinguish between the causes of nonstationarity either as a change in process or change in parameter or both, we need to compare across a wide range of models. However, in this study we focus on a single model to understand what the impacts are of changing the parameter sets according to the future climate regime.

Objectives and scope of study

In this study we propose and evaluate a novel nonstationary uncertainty framework for obtaining streamflow projections under a changing climate. The hypothesis we put forward is twofold:

- The parameters of a given model obtained through calibration on historical records will change in a changing climate and thus, new sets of parameters need to be obtained for simulating future climate scenarios instead of using the parameters obtained by calibration to historical data.
    - To address this issue we adopt the method of 'trading-space-for-time'. It extends the use of regionalization for predicting flow in ungaged basins to predicting flow in a changing climatic scenario. Regionalization [*Yadav et*

al., 2007] involves development of a relationship between a watershed response characteristic and its climatic/physical characteristics.

- The second part of our hypothesis is that, the parameter estimation process does not result in a unique parameter set, but has uncertainty attached to it and that it is important to quantify this uncertainty in order to make more robust decisions.
    - We demonstrate in this paper a way to do this by accepting an ensemble of parameter values satisfying our performance criteria instead of using just one best parameter set.

We introduce this method and demonstrate its application on four watersheds located in climatically different parts of the United States. As introduced earlier, the concept of climate elasticity can be used to quantify the sensitivity of streamflow to climate change. Here, the introduction of uncertainty and nonstationarity provides us with a tool to analyze the climate dependence of streamflow elasticity. We demonstrate how elasticity estimates will depend on how a watershed model is used and also allow for uncertainty in the same. Also, the estimates of elasticity derived from the approach developed in this paper and from the traditional approach are compared in order to reveal the difference in the results obtained.

It has been mentioned earlier that the source of nonstationarity can be both the model used and the parameters. One of the limitations of this study is that we use only one model and therefore focus only on the change of parameters with climate and not on the change of processes within the watershed as the climate changes. Another assumption of the study is that the regression relationships developed for using spatial gradients as a proxy for temporal gradients accurately define how watersheds will change with time.

Chapter 2

Model

It is important to stress that the method introduced here is fully independent of the model used. It can therefore be applied to conceptual or physically-based, lumped or distributed models. The model chosen for this initial study is a typical parsimonious lumped conceptual model with eight parameters (Fig. 1) [*Boyle et al.*, 2000; *Wagener et al.*, 2001]. The model consists of a snow, a soil moisture accounting and a routing module (see Figure 4-1). The snow module accounts for the snow storage and melt. If average temperature is less than a chosen threshold temperature, precipitation is converted to snow, otherwise it falls as rain and directly enters the soil moisture accounting module. Based on *DeWalle and Rango* [2008], the melt equation is given as,

$$M = DDf * (T_{av} - T_b) \quad (3)$$

where, M [mm/day] is the melt at the end of every time step, DDf [mm/day/°C] is the degree day factor, T_{av}[°C] is the average temperature for the day, and T_b[°C] is the base temperature above which melting takes place. The soil moisture accounting module consists of a Pareto distribution of stores that describes the available soil storage in the watershed [Fig. 1; Moore, 2007]. Parameter b [-] defines the soil moisture distribution shape and C_{max} [mm] is the maximum storage in the soil moisture zone. The maximum storage capacity of the watershed, S_{max} [mm], is related to parameters b and C_{max} as

$$S_{max} = \frac{C_{max}}{(1+b)} \quad (4)$$

ER1 [mm/d] and ER2 [mm/d] represent effective rainfall in excess of the storage

capacity that go to the routing module. Quick flow and slow flow are each routed through a single linear reservoir. The model calculates actual evapotranspiration, AE [mm/d], as a linear function of actual soil moisture storage content and of potential evapotranspiration. The model runs at daily time step to account for the variability in snow storage/melt during the month.

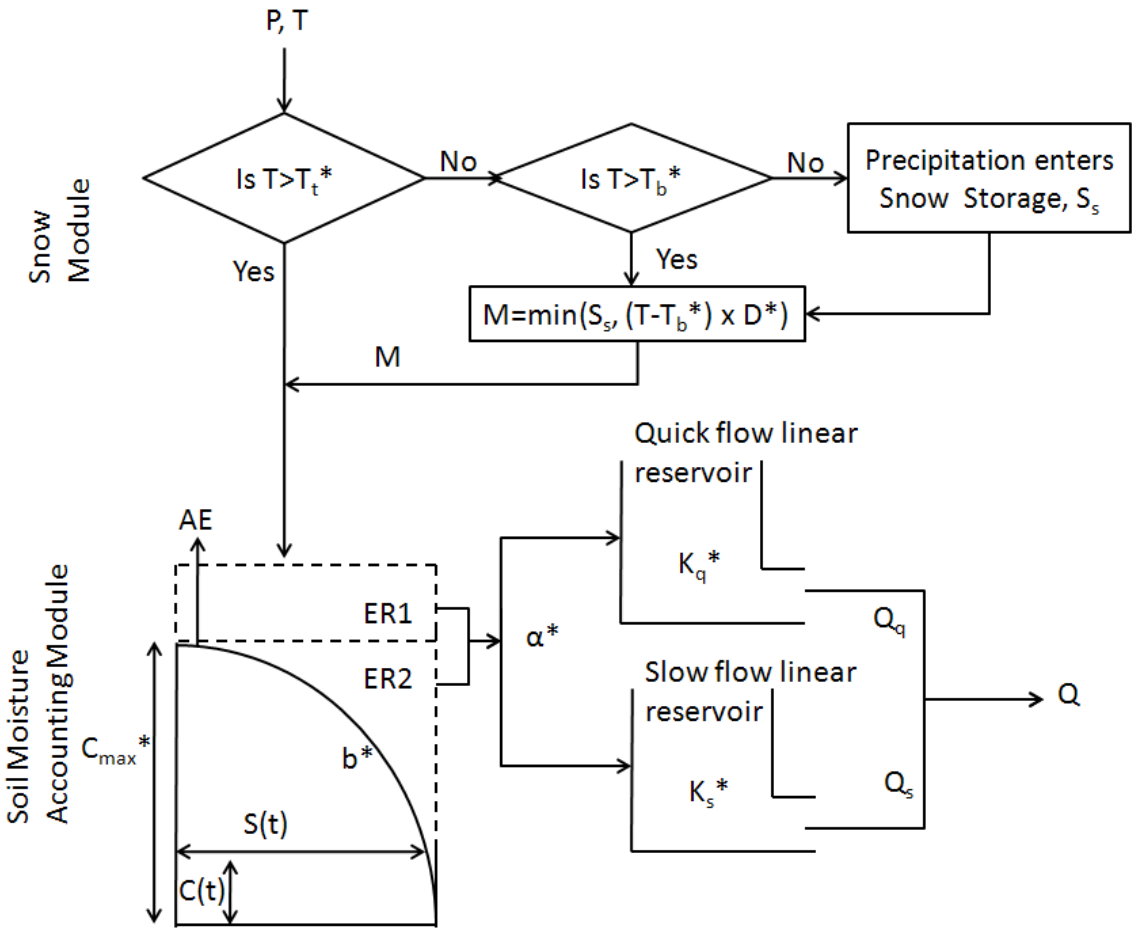

Figure 2-1 The model used in the study combines a snow module with a probability distributed soil moisture accounting module. The model uses a parallel routing scheme for quick and slow flow contributions to streamflow. Q_q, Q_s and AE are model outputs. P and T are precipitation and average daily temperature inputs respectively. T_t^* ,T_b^*, D^*, C_{max}^* ,b^*, α^*, K_q^* and K_s^* are the model parameters.

Chapter 3

Methods

A Nonstationary Uncertainty Framework for Environmental Change Impact Projections

Watershed models and corresponding parameter sets are needed for hydrologic predictions of continuous streamflow in support of a wide range of applications. While most model structures are relatively flexible and can therefore represent a range of watersheds as long as dominant processes are represented by the model, we know that model parameters will change with changing soil types, geology, or land cover [*Hundecha and Bardossy*, 2004; *Buytaert and Beven*, 2009]. We also know that they will change with climatic characteristics [*van Werkhoven et al.*, 2008; *Rosero et al.*, 2010]. Hence for modeling change we need to allow the model parameters to change as a function of changing environmental characteristics [*Wagener et al.*, 2007]. One strategy to do so is to use existing spatial gradients (identified through regionalization) as a proxy for temporal gradients [*Hundecha and Bardossy*, 2004]. Here, we expand the use of the predictions in ungauged basins framework introduced by *Yadav et al.* [2007] to model change impacts, i.e. we move from predictions in ungauged basins (PUB) to predictions in ungauged times (PUT). *Yadav et al.* [2007] introduced a model-independent method to predict streamflow in ungauged basin by developing empirical relationships between the watershed's climatic and physical characteristics and its hydrologic response behavior (i.e. streamflow signatures). These responses were then regionalized in an uncertainty framework to predict streamflow signatures (including uncertainty) of ungauged watersheds. These regionalized signatures contain the information needed to calibrate a hydrological model and therefore allow for a watershed model to be set-up for continuous streamflow simulations at ungauged locations. Including the estimation of the 95% prediction

limits in the regionalization means that acceptable ranges for streamflow signatures can be calculated for ungauged watersheds. Model simulations at the ungauged sites that fall within the limits are acceptable or behavioral, the rest is considered infeasible. The approach to predicting the behavior of a watershed for a future climate scenario is analogous to predicting the same for an ungauged watershed once a regionalized relationship is developed. The aspects of the response behavior that are dependent on climate are the ones for which the spatial gradients can be turned into temporal gradients for a changing climate.

Instead of addressing the two issues of changes in parameter sets with climate and addition of uncertainty estimates separately, we provide a holistic approach to the entire problem by adopting the methodology outlined in this section. First, instead of using calibration on historical records to obtain one 'best' performing parameter set, we define acceptable signature ranges such that every parameter set satisfying our criterion becomes a behavioral parameter set (see Figure 3-1).

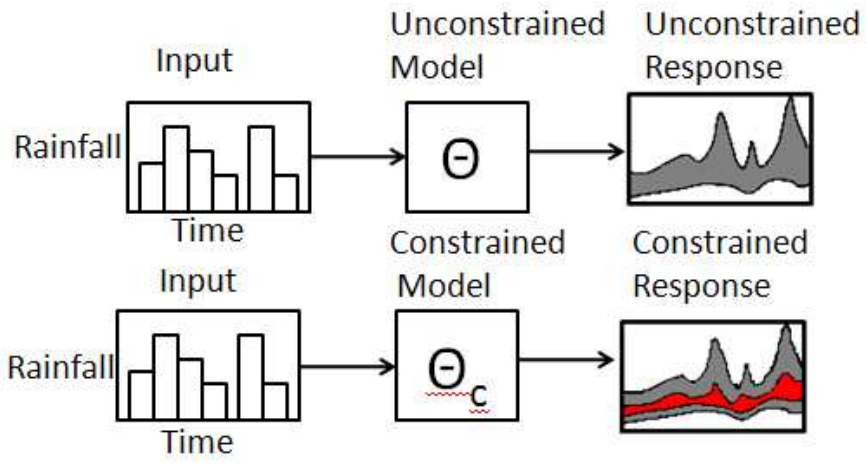

Figure 3-1 The process of constraining response to obtain an acceptable ensemble of parameters.

As signatures we tested different characteristics of the watershed response that explain some of the functional characteristics of a hydrological system [*Wagener et al.*, 2007]. For example runoff ratio (ratio of long-term average streamflow to precipitation) describes how the watershed separates precipitation into streamflow and evapotranspiration, baseflow index (the ratio of quickflow to slowflow) describes differences in flowpaths of water through the watershed, etc. Several such signatures were analyzed in terms of their efficiency in constraining the predicted flow and with respect to their ability for regionalization. Runoff ratio and baseflow index were chosen as the most effective combination for uncertainty reduction while allowing for their regionalization across the close to 400 watersheds included in this study. These response signatures were then regionalized relationships across the entire United States. Uncertainty bounds are applied to the resulting relationship based on the statistical confidence interval and prediction interval to obtain constraints on the expected watershed response for any new value(s) of the predictor(s) (i.e., the climatic/physical characteristics of an ungauged watershed) (see Fig 3-2). For this study, we apply an uncertainty bound by defining 90% prediction limits for every regression model.

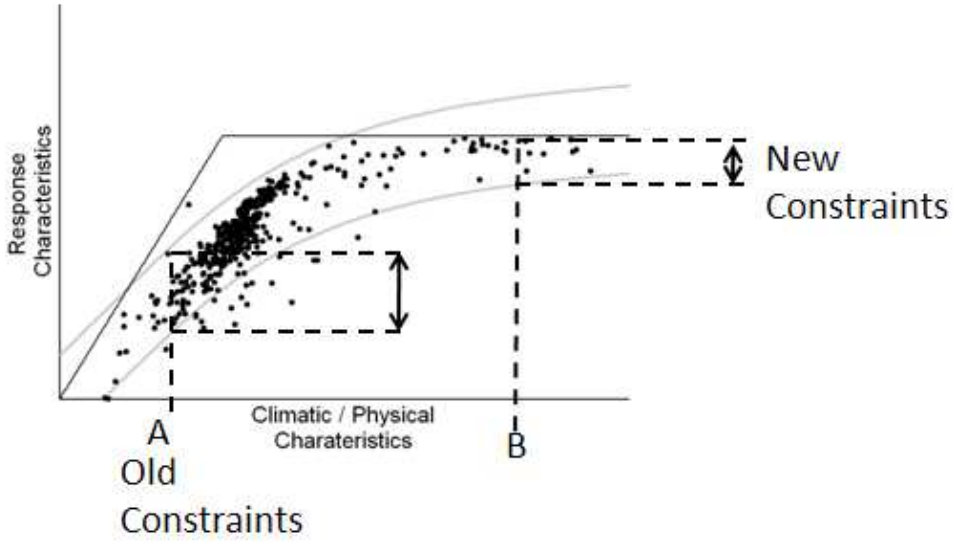

Figure 3-2. Regionalization: Trading-space-for-time. The figure depicts the change of constraints as a watershed moves from climatic region A to climatic region B. This change in

constraints will affect the output flow ensemble predictions. This position is different for historical and prediction periods. Therefore, we can have two types of constraints, one based on the historical relationship between Runoff Ratio and Aridity index which we term as Type A constraint and another based on the changed relationship which we term as Type B constraint. Following this procedure, we derive an acceptable range of signatures for a given climate scenario and each parameter set that produces a value within this range is considered a possible representation of the system.

Chapter 4

Data

Data from 394 watersheds across the United States was used here both for regionalization purposes and for testing of the framework in different climatic regions of the US. Watersheds ranged in size between 66.5 km^2 and 10425 km^2. Time series of hydrologic variables were provided by the MOPEX project at a daily time step [*Duan et al.*, 2006], while physical and average climatic characteristics for all watersheds were obtained from the database provided by *Falcone et al.* [2010]. Potential evapotranspiration was calculated from available temperature data using the Hargreaves equation [*Maidment*, 1993],

$$PE = 0.0023\ S_o\ (T + 17.8)\ \sqrt{\delta_t} \qquad (5)$$

Where T is temperature [° C], δ_T is the difference between mean monthly maximum temperature and mean monthly minimum temperature [° C] (i.e. the difference between the maximum and minimum temperature for the given month, averaged over several years) and S_o is the water equivalent of extraterrestrial radiation [mm d^{-1}] for the location.

Selection of Watersheds for Case Study

The goal of the study is to investigate the impact of changing parameters on the output of future simulations. To demonstrate that the strategy impacts any kind of watershed, we choose watersheds from three different regions of the Budyko curve defined by the aridity index (see Figure 4-1). The aridity index is the ratio of long-term average annual values of potential evapotranspiration to precipitation.

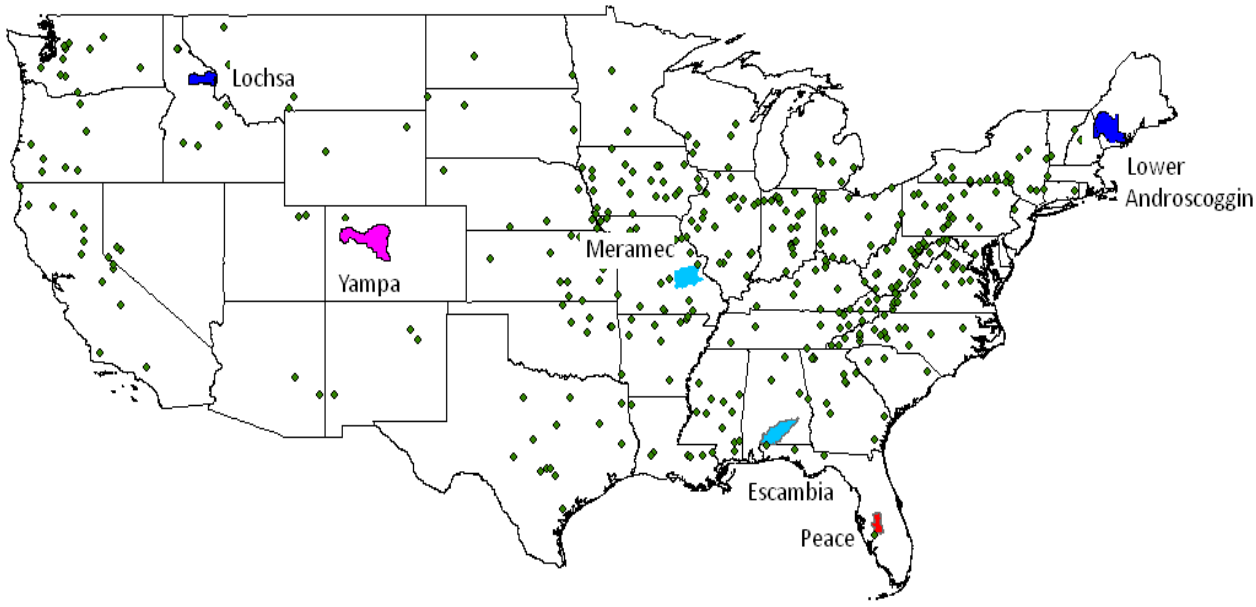

Figure 4-1. Location of the 394 watersheds used for regionalization along with the 6 chosen case study watersheds.

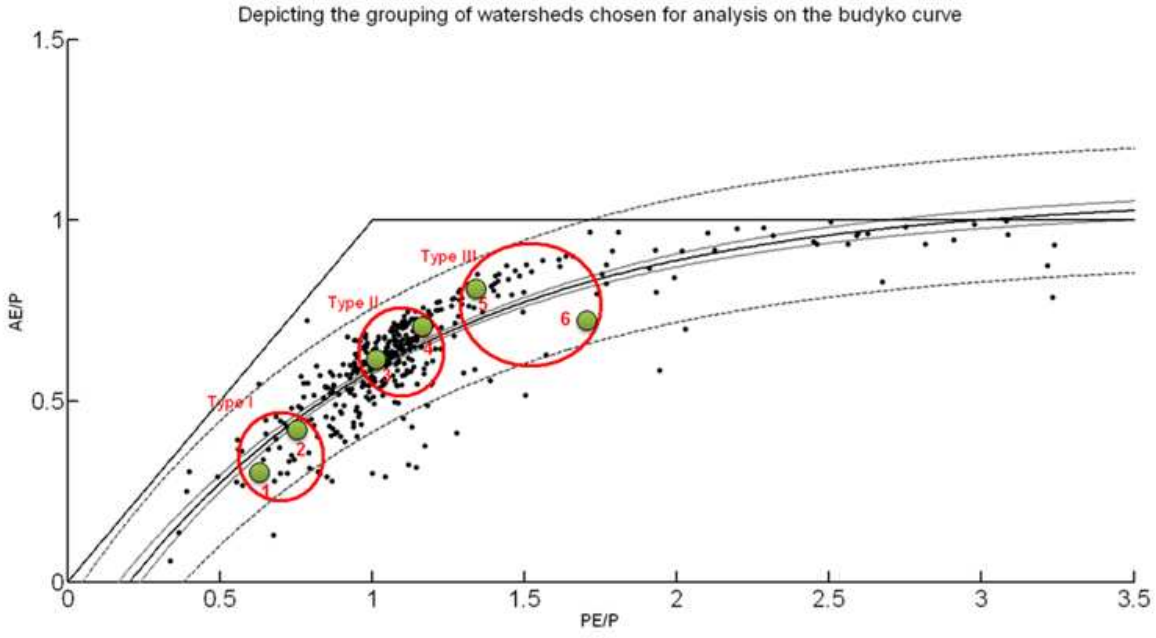

Figure 4-2. Location of selected watersheds on the Budyko curve

The watersheds are categorized:

- Type I Watersheds from the energy limited zone: It is defined as the region in which aridity index <0.8. Two watersheds are selected from this zone: The Lower Androscoggin in Maine/ Newhampshire and the Lochsa watershed. in Idaho/ Montanna
- Type II Watersheds from the region on the division between these 2 zones: The watersheds chosen are the Escambia watershed in Alabama/Florida and the Meramec watershed in Missouri.
- Type III Watersheds from the water limited zone: It is defined as the region in which aridity index >1.2. Two watersheds are selected from this zone: The Peace watershed in Florida and the Yampa watershed in Colorado.

Watershed ID	**Climatic Regime**	**Name of Watershed**	**State**	**Size [km^2]**	**Mean Basin Elevation [m]{Average (range)}**
1055500	Energy Limited	Lower Androscoggin	Maine/ Newhampshire	438	190 (84-651)
13337000	Energy Limited	Lochsa	Idaho/ Montanna	3051	1584 (446-2672)
2375500	Even	Escambia	Alabama/ Florida	9886	95 (10-204)
7019000	Slightly Water Limited	Meramec	Missouri	9811	279 (119-528)
2296750	Water Limited	Peace	Florida	3540	32 (2-89)
9251000	Water Limited	Yampa	Colorado	8832	2364 (1798-3766)

Table 4-1. List of watersheds chosen for the study along with their location, size and mean basin elevation.

Name of Watershed	**Aridity Index (PE/P)**	**% Precipitation as Snow**	**Mean Annual Precipitation [mm/yr]**	**Mean Annual Runoff [mm/yr]**	**Mean Annual PE [mm/yr]**
Lower Androscoggin	0.756	35.7	1149	669	868
Lochsa	0.628	55.2	1330	932	836
Escambia	1.010	0.1	1472	577	1486
Meramec	1.166	10.5	1034	315	1205
Peace	1.331	0	1215	234	1617
Yampa	1.705	47.2	572	159	975

Table 4-2. List of climatic characteristics of the chosen watersheds along with their mean annual runoff.

Chapter 5

Results and Discussion

Testing the value of signatures as constraints

Every response characteristic has an impact on one or more parameters of the model used to represent the watershed. For example, the runoff ratio represents the watershed's annual water budget and therefore impacts the parameters C_{max} and b since it is these two parameters that determine the water budget [*Zhang et al.,* 2008]. The watershed response variables (signatures) considered in this study were: base flow index, recession coefficient, runoff ratio and slope of the flow duration curve. These were used individually and in their combinations with the runoff ratio to analyze the efficiency of constraining which was determined by using two indicators: sharpness and reliability [*Yadav et al.*, 2007; *Zhang et al.*, 2008]. The response criterion, which performed best for both sharpness and reliability was a combination of RR and BFI. See Appendix B for detailed results.

Regionalization of signatures

Once signatures have been chosen, they were regionalized to formalize spatial variability.

- Regionalization of Runoff Ratio:

Previous studies have indicated that the runoff ratio has a strong relationship with the aridity index [*Dooge et. al*, 1992]. Different equations by Turc-Pike, Ol'dekop and Schreiber were used to regress runoff ratio with aridity index for the 394 watersheds across US [for equations see *Dooge et al.*, 1992]. The Schreiber relationship provided the best fit for the watersheds under study and was subsequently used. Appendix C lists the results using the other two equations. The Schreiber relationship is:

$$\frac{AE}{P} = 1.0657 - 1.3068 * \exp\left(-\frac{PE}{P}\right) \qquad (6)$$

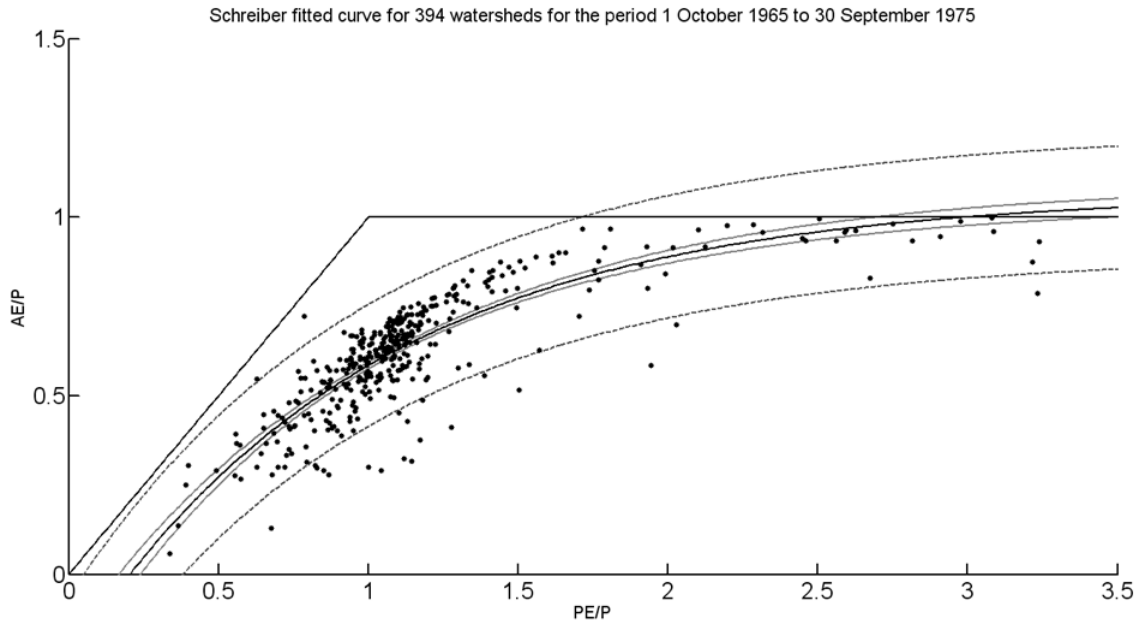

Figure 5-1. Regionalized Schreiber relationship between AE/P (1-Q/P) and aridity index PE/P. Here Q is the mean annual flow, P is the mean annual precipitation, AE is the mean annual actual evapotranspiration and PE is the mean annual potential evapotranspiration for the period 1 October 1065 to 30 September 1975.

- Regionalization of baseflow index:

Using data from 394 watersheds across the United States, the dependence of base flow index on various physical and climatic characteristics of the watershed was quantified. The correlation between baseflow index and a multitude of watershed characteristics was evaluated using the spearman coefficient. The results indicate that baseflow index is highly correlated (Spearman coefficient >0.5) with percentage of soils in the variable drainage characteristics, average permeability, average value of sand content (percentage), average K-factor value for the uppermost soil horizon in each soil component, riparian 100m buffer percent perennial ice/snow and watershed percent perennial ice/snow. The value of spearman coefficient for precipitation and potential evapotranspiration are 0.03 and 0.25 respectively. Based on these values, it was assumed in this study that base flow index does not change with climate and historical behavior of the watershed can be retained when modeling future scenarios.

Application of methodology for assessing climatic scenarios

IPCC summary results provide estimates of expected change in precipitation and temperature for the United States [*Christensen et al.*, 2007]. For precipitation the maximum expected change ranges between -30 % to +40 % whereas a rise of about 8 °C is the maximum expected temperature change during the 21st century. No decline in temperature was considered as a feasible scenario. Guided by these ranges, we developed a matrix of temperature and precipitation change, with the precipitation change of 10% per step and a temperature rise of 1°C for each step, according to the ranges identified above. New time-series of changed climate are obtained by changing the mean precipitation and mean temperature for a ten-year historical period, and by using this changed time-series as model forcing. Hence we only change the mean and assume that the remaining characteristics of precipitation and temperature remain the same. This assumption is similar to many studies including *Nash and Gleick* [1991], *Jones et al.* [2006] and *Jiang et al.* [2006]. More sophisticated scenarios will be tested at a later stage.

Change in constraints with changing climate

Once the climatic scenarios are defined, we obtain constraints related to each scenario for each watershed. We define the constraints in the following manner:

- Type constraints A: Those that are derived from historical observations.
- Type constraints B: Those that are derived from the changing climatic conditions.

(Behavioral) Population size after constraints: A Monte Carlo analysis was used to generate 10,000 sets of model parameters in which we assumed uniform distributions for all parameters and no interactions (a typical approach). The required response signatures (RR and BFI) were calculated for each parameter set. The generated simulations were 'filtered' using the two types of constraints, thus two types of accepted model ensembles were arrived. Remember that only runoff ratio will change with a changing climate, therefore, only this constraint on the water balance was changed. Note that there is only one type A ensemble but there are multiple type B ensembles (equal in number to the

number of climatic scenarios considered). Finally, using this approach, we arrive at different ensemble predictions of streamflow which are analyzed in the results section.

Matrix of ensemble streamflow predictions

A matrix of ensemble streamflow predictions was developed in order to compare the two types of constraints. Figure 5-2 depicts how the constraints were derived.

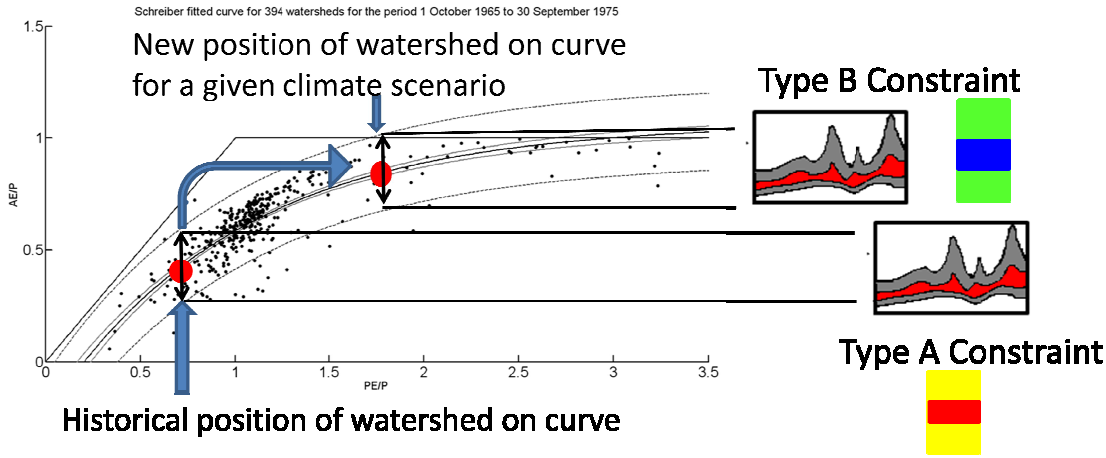

Figure 5-2. Derivation of Type A and Type B constraints from the Budyko curve.

For every climatic scenario considered, we can derive a constraint based upon the position of the watershed on the Budyko curve. There is one constraint which is based on the historical position of the watershed on the curve. This constraint give us the Type A constraint which can be used to generate the historical ensemble of parameter sets. Now for every new climatic scenario, we have two options:

- Use parameters derived from Type A constraints: This is the historical parameter set and the output from using this parameter set is given by yellow and red rectangles, yellow for prediction interval and red for confidence interval.
- Use the parameters derived from Type B constraints: This is the new parameter set for the new climate scenario and the output from this parameter set is given by green and blue rectangles, green for prediction interval and blue for confidence interval.

For both the Type A and Type B outputs, the upper edge of the rectangle gives the maximum predicted flow and the lower edge of the rectangle gives the minimum predicted flow. Therefore, the rectangle represents the ensemble of flows that are expected in the given climatic scenario.

Figure 5-3 describes how the results are plotted upon the output matrix of precipitation and temperature. The x-axis represents the increase in temperature and the y-axis represents the changes in precipitation. Each grid box, therefore, represents a combination of change in precipitation with temperature. The two types of constraints derived from the Budyko curve can then be plotted side by side as shown in the figure 5-3. In this particular figure, the constraints are plotted for a no-change scenario, therefore both the results are exactly the same. Every horizontal line in the matrix is the historical mean annual flow and therefore the position of the rectangle with respect to the horizontal line gives us an idea of the change in the mean flow for that climate scenario with respect to the historical mean flow. The length of the rectangle gives an assessment of uncertainty associated with the prediction.

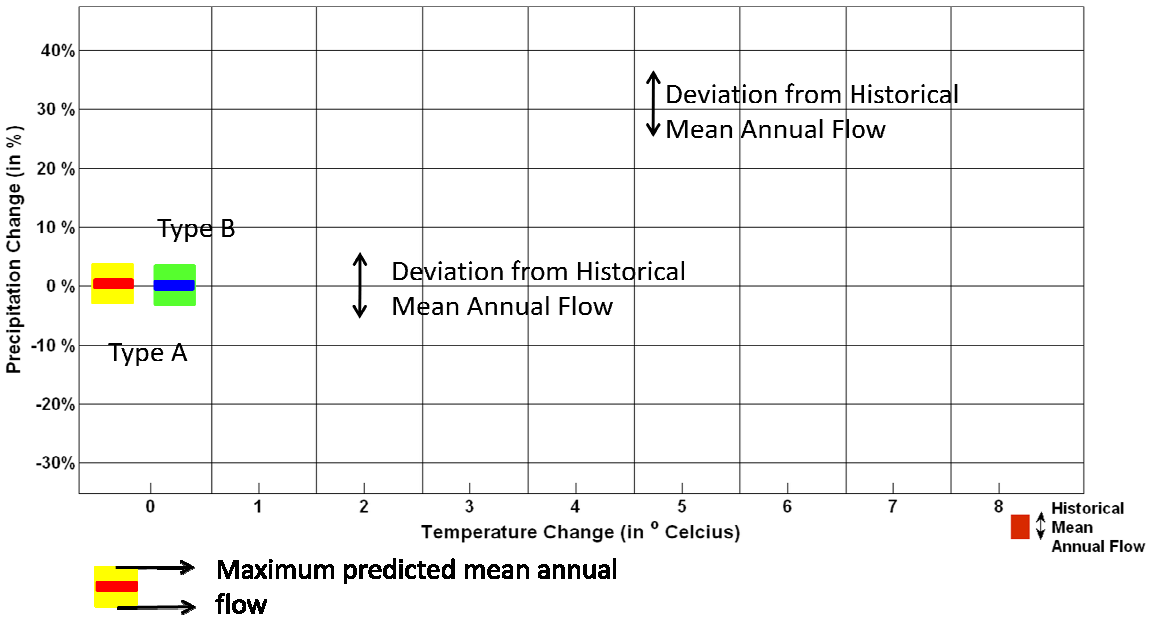

Figure 5-3. Explanation of the output flow matrix. The red box in the lower right gives an estimate of the scale of the plot.

The matrix in Figure 5-4 (a-f) shows that as we move away from the historical climate, the difference between the predictions of Type A and Type B ensembles increases for the following cases:

- Increase in temperature only (and precipitation range smaller than historical to slightly greater than historical): The Type B ensemble predicts increasingly smaller values of flow and the predictions become increasingly more constraint.
- Decrease in precipitation only: Shows the same trend as with the historical constraints.
- Increase in temperature, decrease in precipitation: show the same trend as before.

These three trends are observed quite similarly in all the watersheds. The aforementioned trends are explainable if we consider how the watershed is moving along the Budyko curve for each case. For an increase in temperature only, or for a decrease in precipitation or a combination of both, the ratio PE/P increases and deviates from historical ratio. As we start from PE/P=0, width of the intervals slightly decrease as the curve reaches the information dense area between PE/P=1 and PE/P=1.5, after this it the width starts to increase as we move towards the information sparse region. But at PE/P=1.71, the curve reaches AE/P=1 which is the physical maximum for AE/P. Therefore, after this point, the upper bound remains the same and the lower bound continues to rise, leading to a further decrease in width. For watersheds in energy limited zones or medium zones (low values of PE/P), an increase in PE/P is required so that the watershed climate reaches a value of 1.71. Therefore, for an increase in temperature, a decrease in precipitation or a combination of both will eventually lead to thinning of the ensemble predicted from Type B, this thinning will be most pronounced for a combination of the two scenarios.

For water limited zones, we start off very near to PE/P=1.71, therefore the state of AE/P=1 is quickly reached, the band thins down and then remains constant for most parts of the temperature-precipitation-change matrix. For the case of an increase in precipitation, we are decreasing PE/P, hence moving towards the left in the Budyko curve. This means the width of the band will first increase after it crosses the PE/P=1.71 and then more or less remain the same.

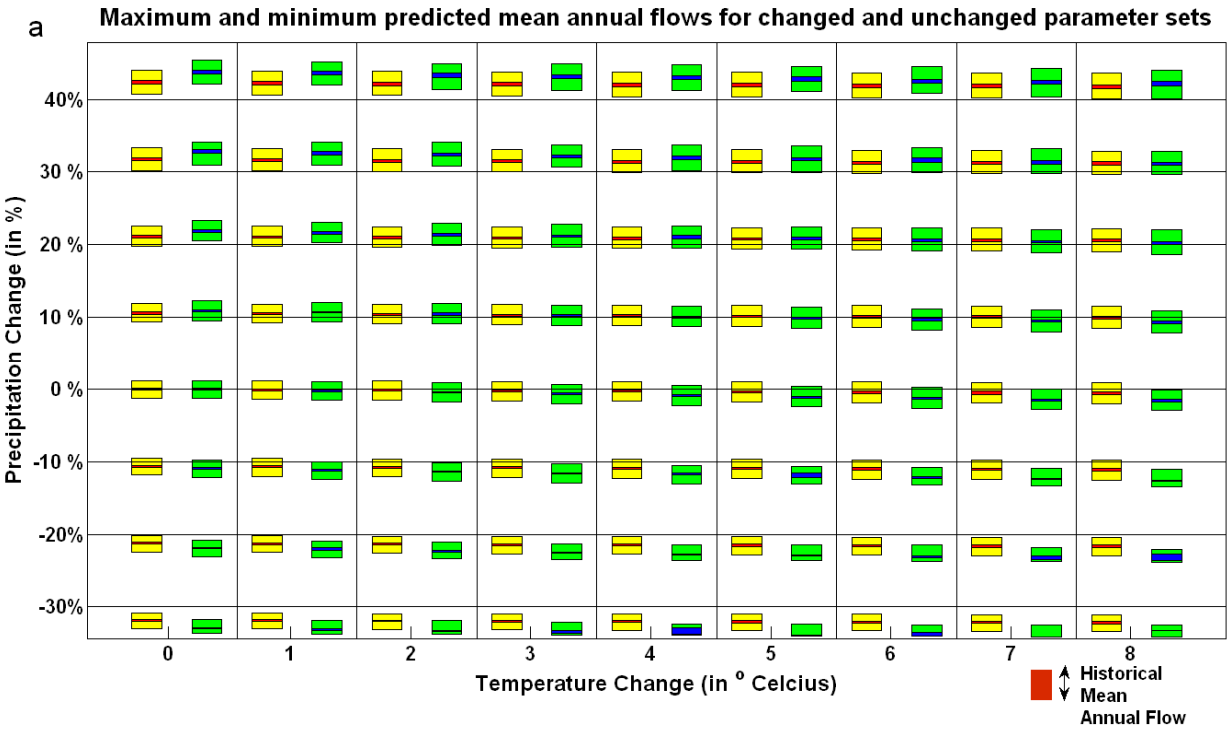
a
Maximum and minimum predicted mean annual flows for changed and unchanged parameter sets
Precipitation Change (in %)
40%
30 %
20 %
10 %
0 %
-10 %
-20%
-30%
0
1
2
3
4
5
6
7
8
Temperature Change (in ° Celcius)
Historical
Mean
Annual Flow

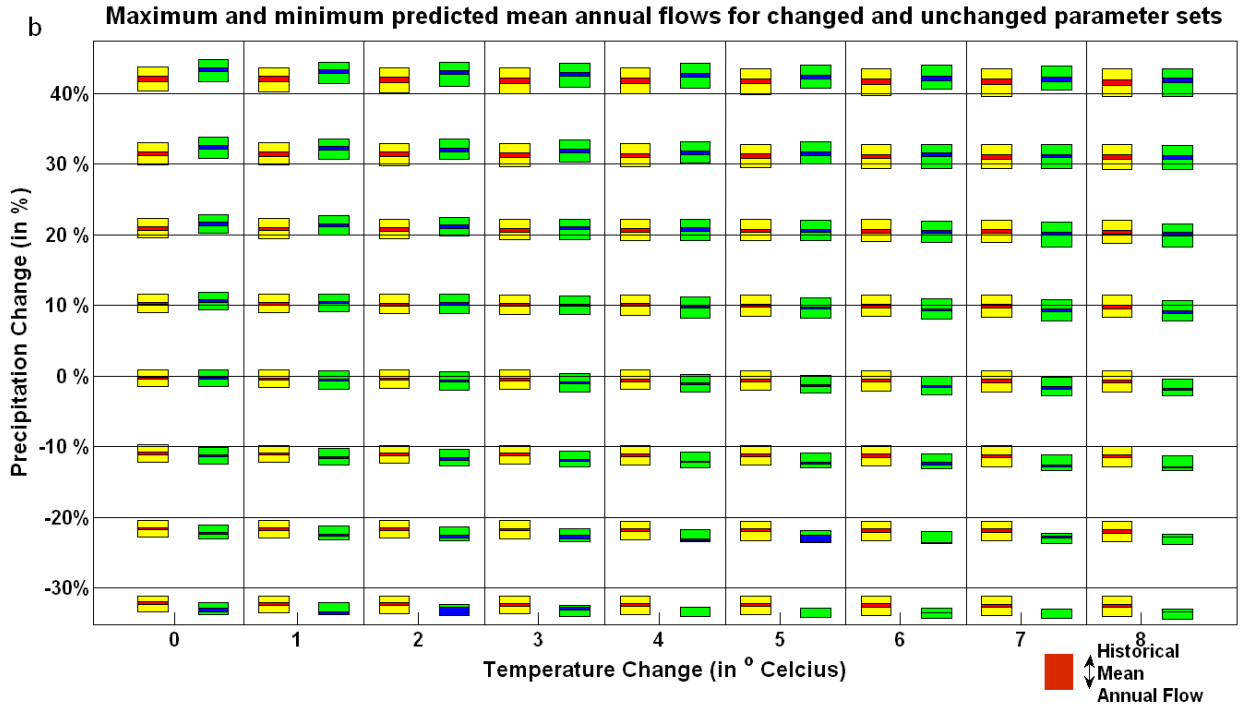
b
Maximum and minimum predicted mean annual flows for changed and unchanged parameter sets
Precipitation Change (in %)
40%
30 %
20 %
10 %
0 %
-10 %
-20%
-30%
0
1
2
3
4
5
6
7
8
Temperature Change (in ° Celcius)
Historical
Mean
Annual Flow

c

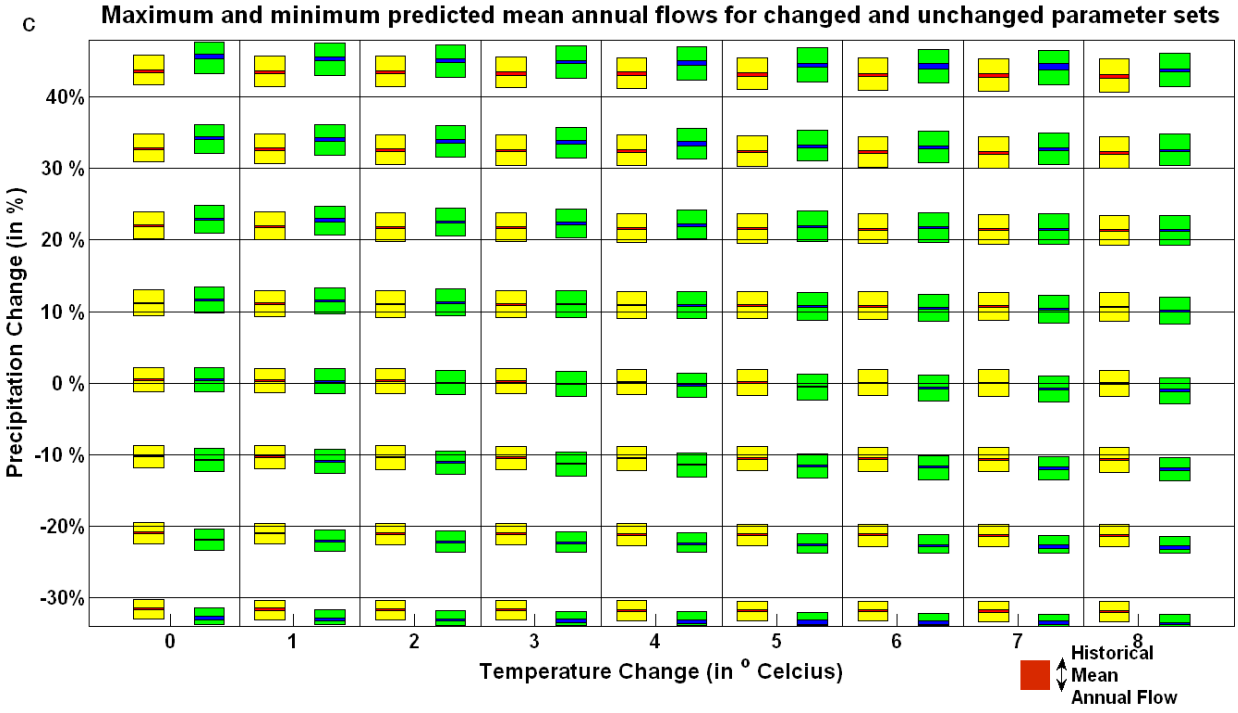
Maximum and minimum predicted mean annual flows for changed and unchanged parameter sets
Precipitation Change (in %)
40%
30 %
20 %
10 %
0 %
-10 %
-20%
-30%
0
1
2
3
4
5
6
7
8
Temperature Change (in ° Celcius)
Historical
Mean
Annual Flow

d

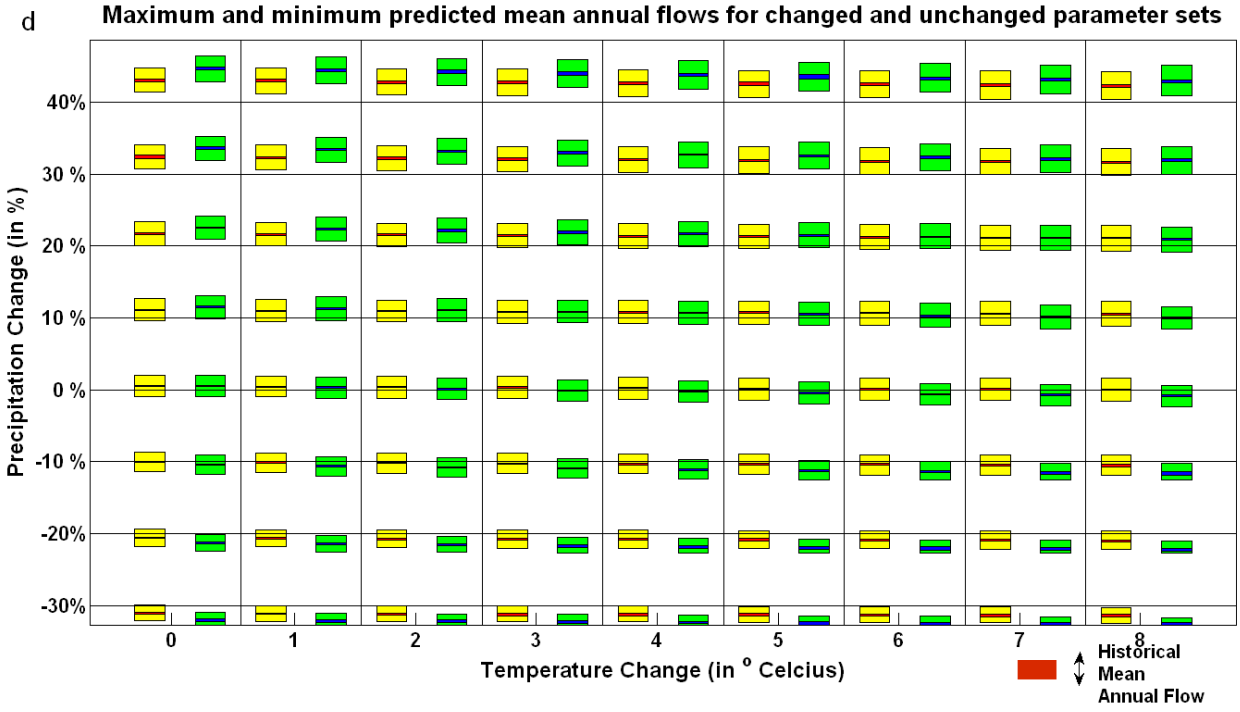
Maximum and minimum predicted mean annual flows for changed and unchanged parameter sets
Precipitation Change (in %)
40%
30 %
20 %
10 %
0 %
-10 %
-20%
-30%
0
1
2
3
4
5
6
7
8
Temperature Change (in ° Celcius)
Historical
Mean
Annual Flow

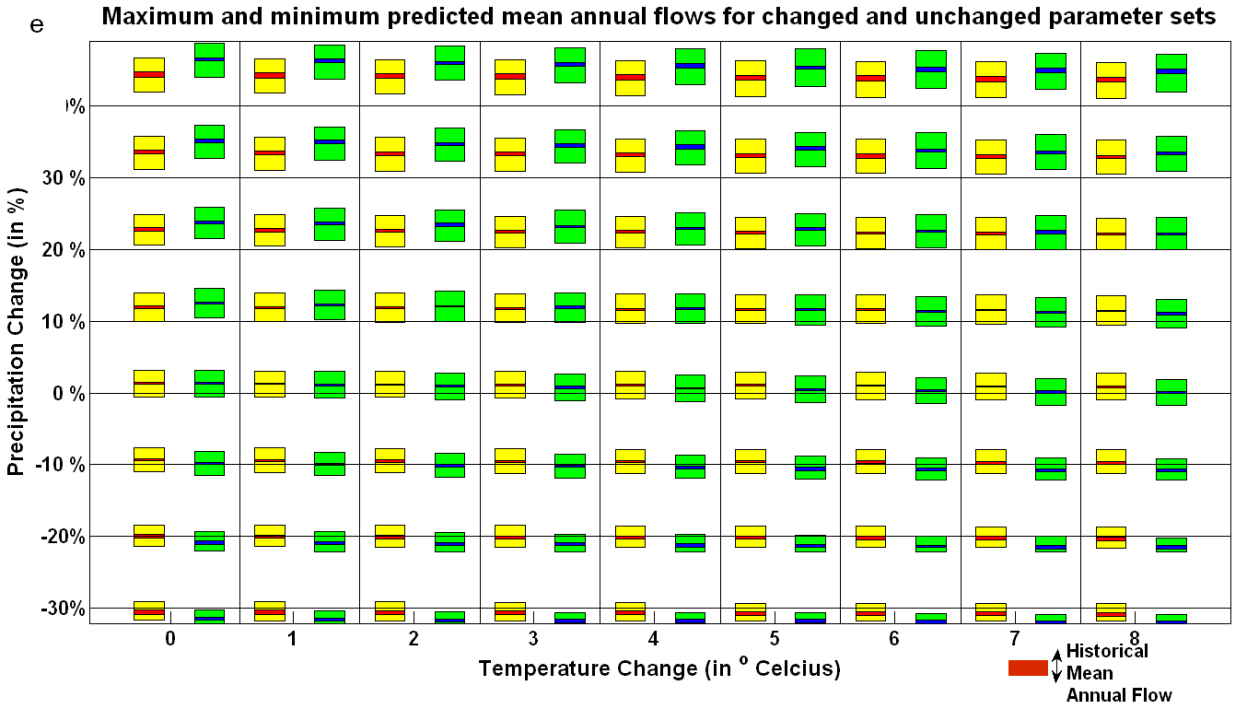

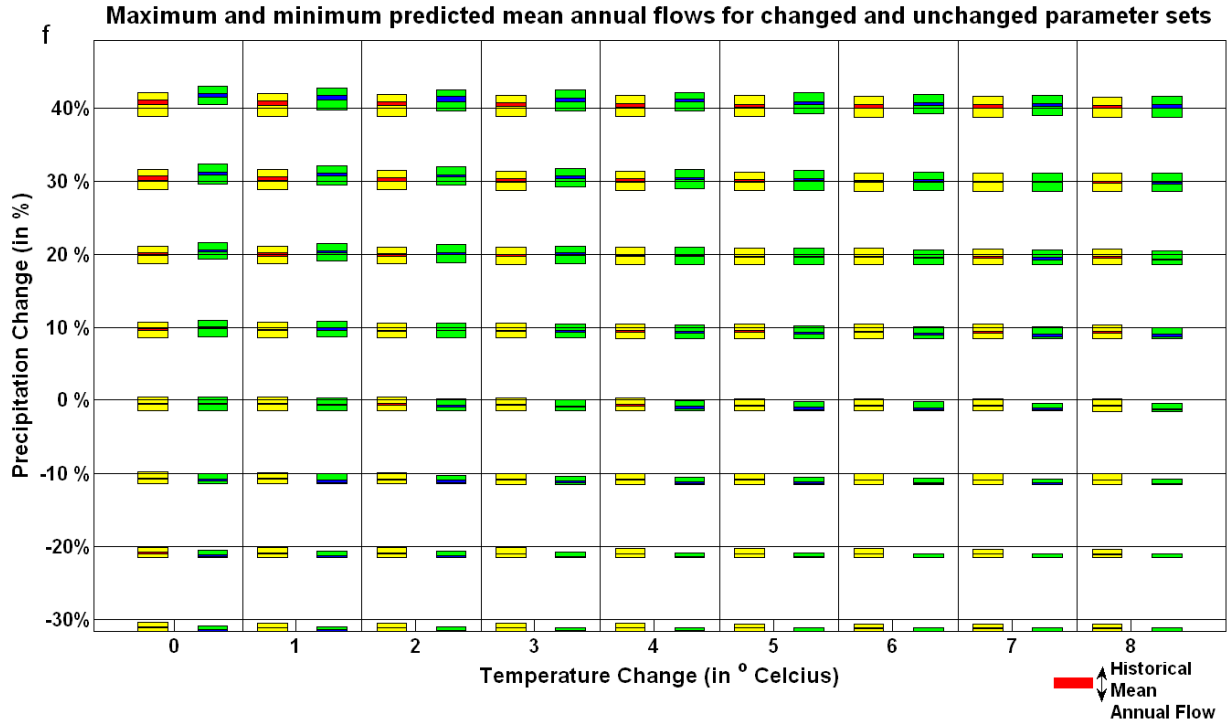

Figure 5-4 (a-f). Matrix of ensemble flow predictions for Type A and Type B ensembles for study watersheds. The yellow and red boxes depict the prediction limits and confidence limit respectively for Type A ensemble. The green and blue boxes depict the prediction and confidence limits respectively for Type B ensemble. The figures are ordered as: (a) Lower Androscoggin, (b) Lochsa, (c) Escambia, (d) Meramec, (e) Peace and (f) Yampa watersheds.

The plots show that for a temperature change of upto 2 °C and for precipitation changes of -10% to +10%, the two approaches produce more or less equal ensembles. Also, as we increase both temperature and precipitation, the change between the ensembles decreases. For example for the Lower Androscoggin watershed, if we increase the precipitation by 20% the two ensembles the predictions become similar for the temperature rise of 5°C to 8°C. For an increase of 30% in precipitation, the two ensembles become similar for a temperature increase of 6°C to 8°C. For an increase of 40% in precipitation, the two ensembles become equal at the temperature rise of 8°C. This trend is seen in all the watershed but the ranges for different watersheds are different. For example, the Lochsa watershed behaves similar to Lower Androscoggin. The Escambia , Meramec and Peace watersheds show a similar trend. The Type A and Type B ensembles become equal for a high temperature rise of the order of 7-8°C and a precipitation increase of 20-30%, but after the precipitation increases beyond 30%, the ensembles are different no matter what the temperature rise. For a decrease in precipitation, the two ensembles always produce different results. The difference is more pronounced when the precipitation decrease beyond 10% and the temperature rises.

These observations are similar to those obtained by *Vaze et al.* [2009] for a study in Australia to quantify the effects of changing climate on the model predictions. They concluded that :

> "lumped conceptual rainfall-runoff models calibrated over an average or wet climatic period are not suitable for simulating runoff over short dry periods, for which the difference in mean annual rainfall is greater than 15 percent. The results also show that rainfall-runoff models calibrated over an average or wet climatic period are suitable for simulating runoff over short wet periods provided the difference in mean annual rainfall is less than 20 percent."

There is a similarity between their results and those obtained from this study, where we find that dry periods always produce different ensembles for the two approaches than wet periods. For wet periods, we find that the two ensembles may/may not be different given the combination of precipitation increase and temperature increase.

Comparison of Matrix for different watersheds

Snow versus No Snow

One striking feature of the plots is that the difference between Type A and Type B ensembles becomes negligible in the extreme scenario of high precipitation and high temperature. Moreover, the difference almost completely vanishes for snow-dominated watersheds. This is related to the calculation of potential evapotranspiration for snow watersheds. Because of a significant number of days with negative temperatures, snow watersheds, have many days with zero values of PE during historical climate. But in the future, as temperatures rise and most of the temperature becomes positive, the watershed reaches a state where PE becomes positive for almost all days. This means, that the increase in PE for a watershed with snow is more than that for one with no snow in which it was simply a function of how much temperature increased. This implies that change in the ratio PE/P is different for snow and no snow watersheds, for a watershed with historical snow, the increase in PE is larger and matches the increase in P, reaching a state where the ratio remains similar to the historical one. In watersheds without significant snow, the relative increase in PE is not able to compensate the increase in P; therefore, the ratio of PE/P is smaller, resulting in smaller values of AE/P and therefore higher runoff ratios. A higher runoff ratio means that the Type B ensemble will predict a higher value of flow than type A, which is consistent with the observation.

Dry versus Wet

The dry climates with high PE/P ratio reach the stage $PE/P > 1.71$ very quickly or even start off from that stage. Therefore, with changes in P and PE that would increase PE/P, the width of predictions for these watersheds reaches a small constant value very quickly. Not only the width becomes constant, the predictions of low flows also become more or less constant across increase in temperatures or decrease in precipitation. This simply means that the watershed reaches a point where the available moisture is evaporated and there can be no further evaporation increase. Therefore a

further rise in temperature or decline in precipitation will not affect the minimum flows anymore. These effects become less and less prominent as the watersheds become wetter.

Elasticity of streamflow

To evaluate the above-define streamflow elasticity, we consider two ways of looking at changes in streamflow to changes in P and T. In the first approach we look at the surface of Q/Q_{hist}, i.e., ratio between the mean prediction of Q for a given climate scenario and the historical value of predicted Q. This historical mean value is not the observed historical mean, but it is the model predicted historical mean, since we want to analyze the impact of using different constraints specifically and not the impact of using the same model for different watersheds. The plots show a general trend that the Type B ensemble surface displays a greater slope than the Type A ensembles. Type B ensembles therefore produce more extreme results than Type A ensembles do. This is clear a direct consequence of accounting for the change in watershed response behavior with changing climate by changing the constraints. Another significant observation is that the difference between the two predictions is far greater for the drier climates than for the wet climates. This has been already explained in terms of the shift of the watershed along the Budyko curve.

Figures 5-3 (a-f) are variations of Q/Q_{hist} with ΔT and ΔP. The value of Q is taken as the mean of the predicted ensemble. The prediction of ratio of mean Q/Q_{hist} is compared for Type A (unchanged) and Type B (changed) parameters. For simplicity, no other detail is added to the plot.

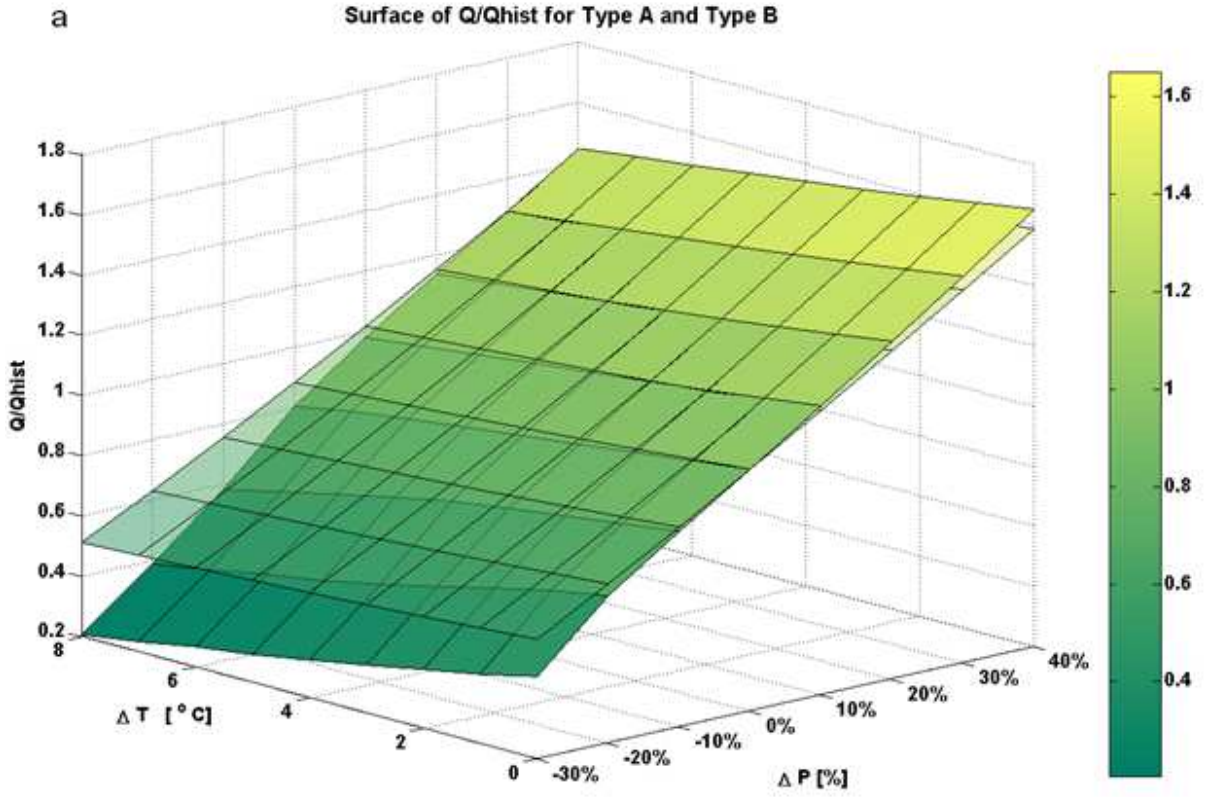
a
Surface of Q/Qhist for Type A and Type B
Q/Qhist
1.8
1.6
1.4
1.2
1
0.8
0.6
0.4
0.2
8
6
4
2
0
ΔT [°C]
-30%
-20%
-10%
0%
10%
20%
30%
40%
ΔP [%]
1.6
1.4
1.2
1
0.8
0.6
0.4

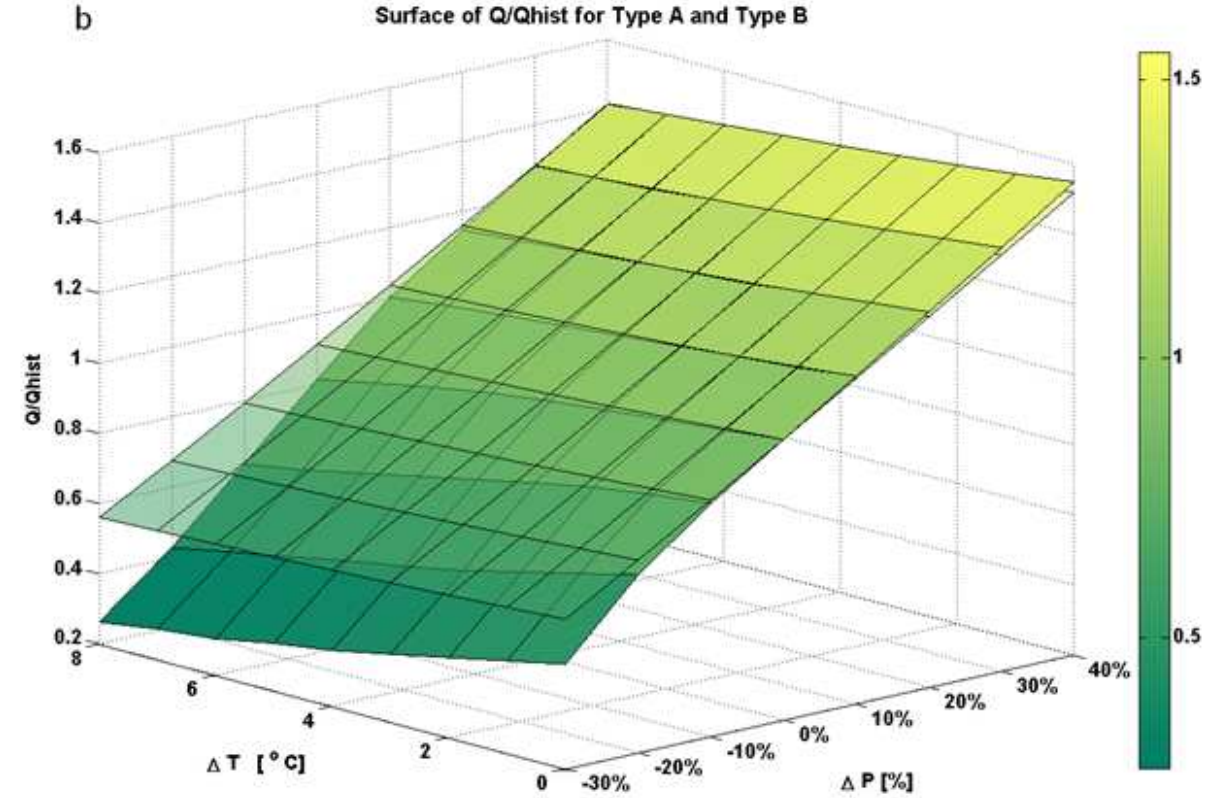
b
Surface of Q/Qhist for Type A and Type B
Q/Qhist
1.6
1.4
1.2
1
0.8
0.6
0.4
0.2
8
6
4
2
0
ΔT [°C]
-30%
-20%
-10%
0%
10%
20%
30%
40%
ΔP [%]
1.5
1
0.5

c

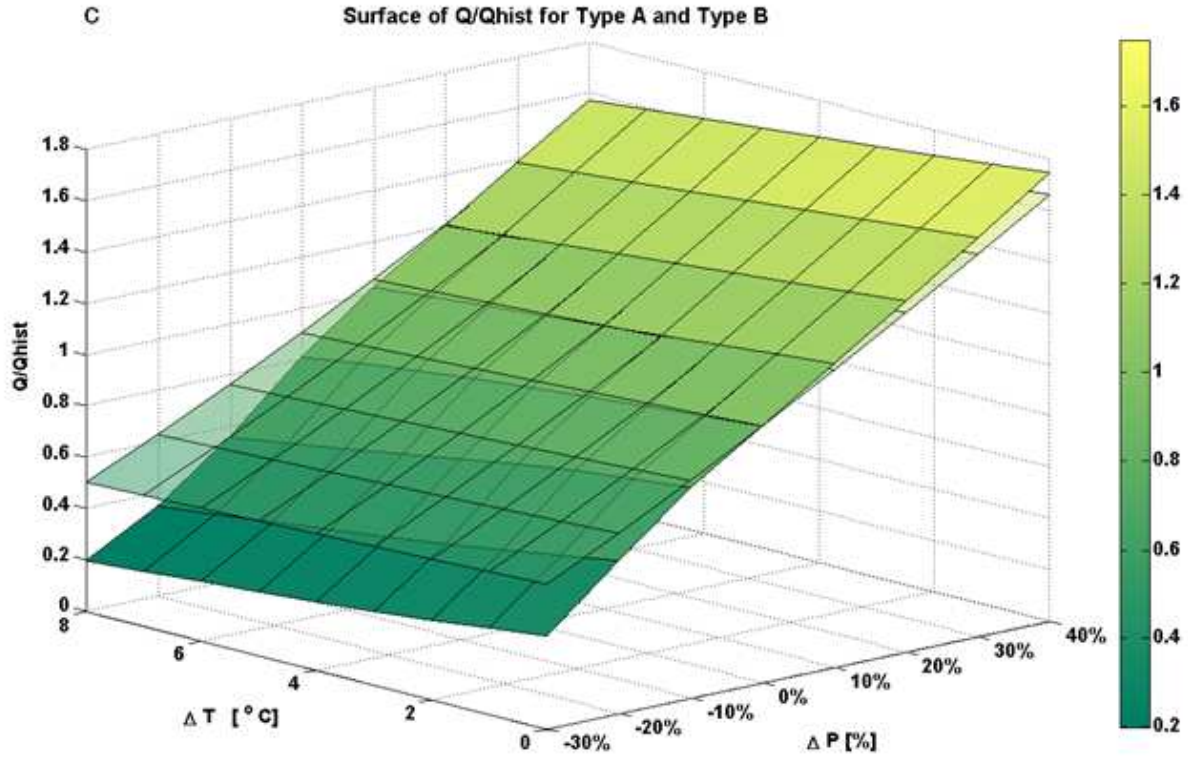
Surface of Q/Qhist for Type A and Type B
Q/Qhist
1.8
1.6
1.4
1.2
1
0.8
0.6
0.4
0.2
0
8
6
4
2
0
ΔT [°C]
-30%
-20%
-10%
0%
10%
20%
30%
40%
ΔP [%]
1.6
1.4
1.2
1
0.8
0.6
0.4
0.2

d

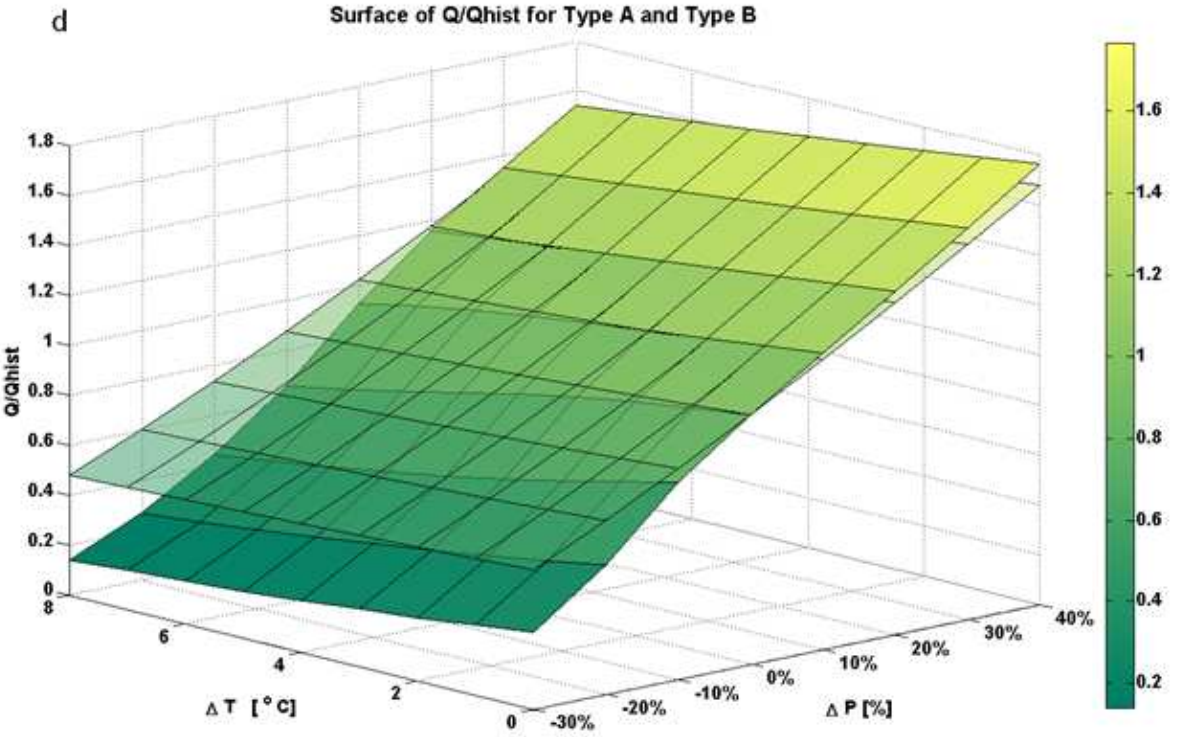
Surface of Q/Qhist for Type A and Type B
Q/Qhist
1.8
1.6
1.4
1.2
1
0.8
0.6
0.4
0.2
0
8
6
4
2
0
ΔT [°C]
-30%
-20%
-10%
0%
10%
20%
30%
40%
ΔP [%]
1.6
1.4
1.2
1
0.8
0.6
0.4
0.2

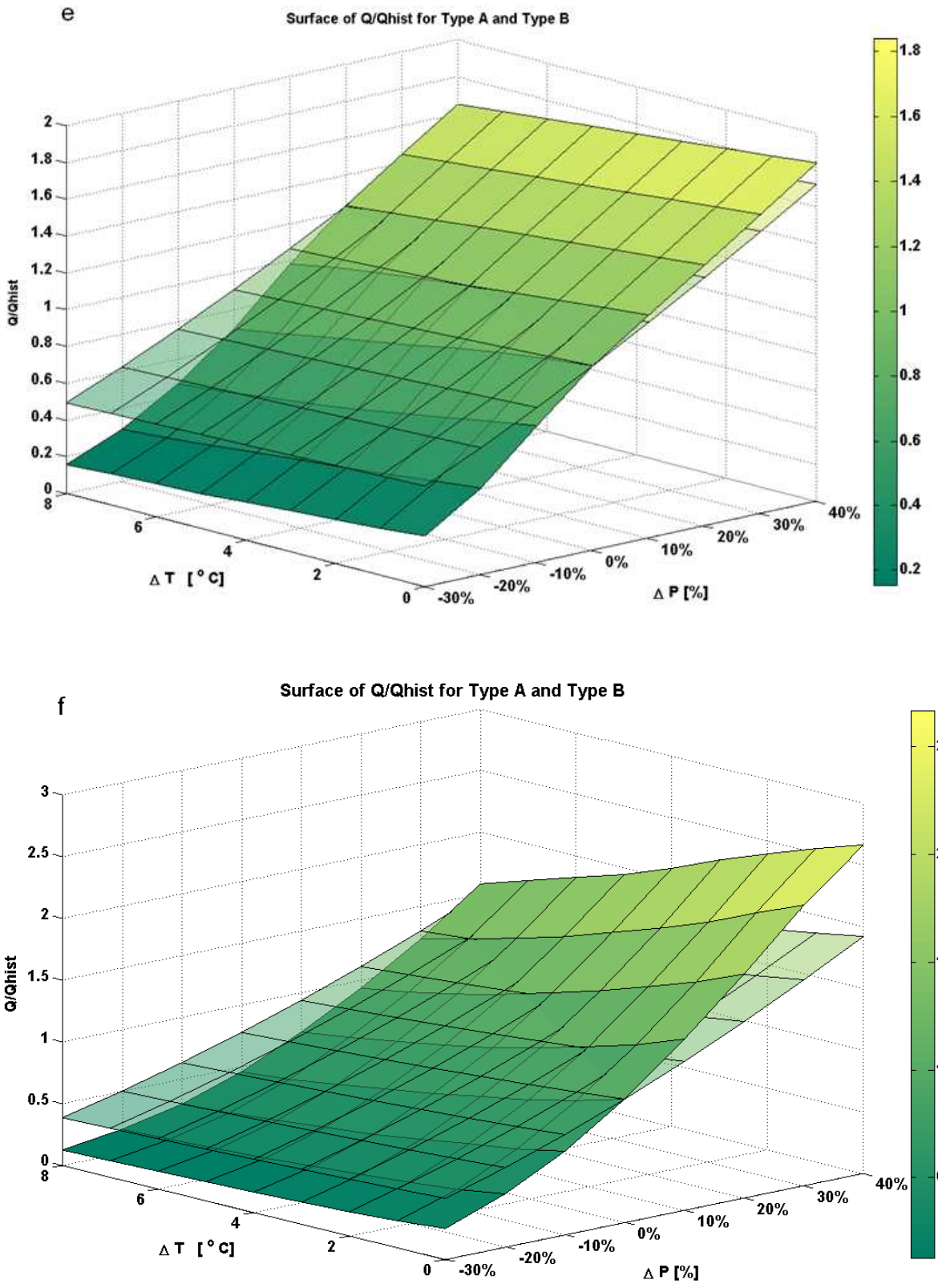

Figure 5-5 (a-f). Surface plot of deviation of mean of ensemble flow predictions for a given climate scenario from mean of the historical ensemble predictions Q/Qhist (Qhist is the mean of the ensemble for no change in temperature or precipitation scenario). The semi transparent

surface plot is of Type A parameter ensemble and the opaque surface plot is of Type B parameter ensemble. The figures are ordered as: (a) Lower Androscoggin, (b) Lochsa, (c) Escambia, (d) Meramec, (e) Peace and (f) Yampa watersheds.

The Yampa watershed produces a surface, which displays a different trend from all other watersheds (Fig. 5-3, f). It shows similar amount of change in the ratio for both an increase and decrease of temperature, though in opposite directions. This happens because it is a dry watershed with a very high percentage of snow (47.2%). The mean annual Precipitation 572 mm, mean annual runoff is 159 and mean annual PE is 975 mm. The high percentage of snow implies that around 270 mm of precipitation falls as snow that is stored in snowpack and released during the melt season. The mean annual runoff is even lower than the total expected melt. The high value of PE indicates losses due to evaporation during the summer season are very significant. An increase in temperature leads to conversion of all snow events to rainfall events, which changes the timing of runoff. The runoff, which previously occurred during spring after snowmelt will now occur during the winter itself, which reduces the loss due to evapotranspiration. So the increase in runoff is more pronounced than in other watersheds.

Contours of Change in Streamflow

The contour plots are plotted using the same concept as the surface plots: they are contours of Q/Qhist with ΔT and ΔP. On the background in these plots we have contours of width of band = Q_{max}-Q_{min} for the given scenario. This gives a sense of uncertainty along with the general trend of change in flow for the two types. The background contours are normalized with respect to the width of the band for the historical ensemble. This allows for ease in comparison across catchments.

a

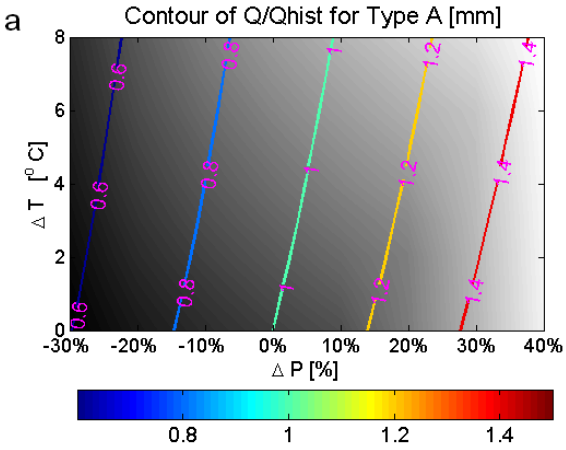
Contour of Q/Qhist for Type A [mm]
Δ T [^{0} C]
Δ P [%]
-30% -20% -10% 0% 10% 20% 30% 40%
0 2 4 6 8
0.8 1 1.2 1.4
Variation in Q/Qhist

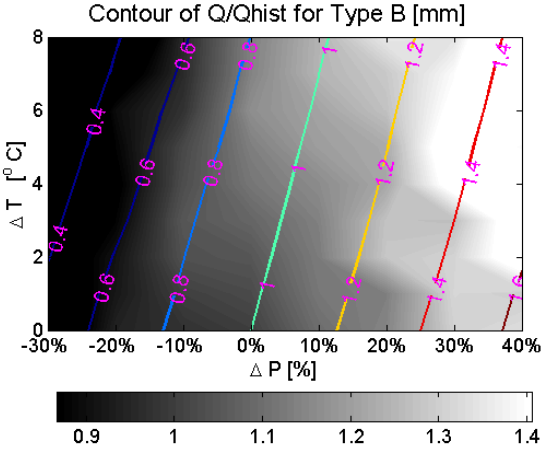
Contour of Q/Qhist for Type B [mm]
Δ T [^{0} C]
Δ P [%]
-30% -20% -10% 0% 10% 20% 30% 40%
0 2 4 6 8
0.9 1 1.1 1.2 1.3 1.4
Variation in width of the band (normalized with respect to the mean of the historical flow ensemble)

b

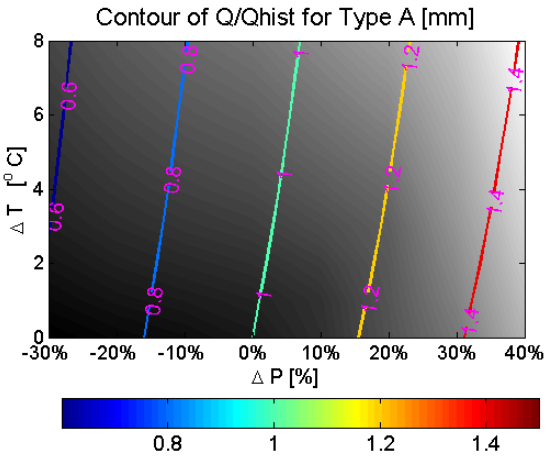
Contour of Q/Qhist for Type A [mm]
Δ T [^{0} C]
Δ P [%]
-30% -20% -10% 0% 10% 20% 30% 40%
0 2 4 6 8
0.8 1 1.2 1.4
Variation in Q/Qhist

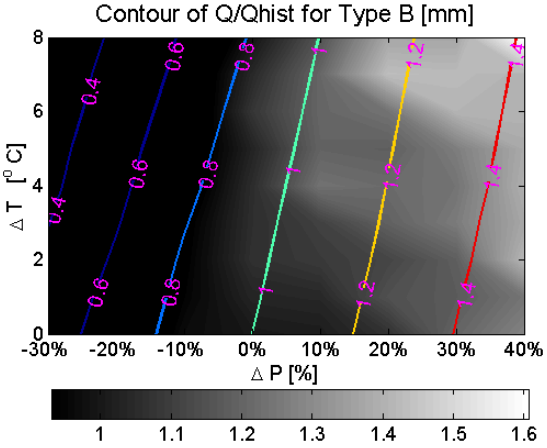
Contour of Q/Qhist for Type B [mm]
Δ T [^{0} C]
Δ P [%]
-30% -20% -10% 0% 10% 20% 30% 40%
0 2 4 6 8
1 1.1 1.2 1.3 1.4 1.5 1.6
Variation in width of the band (normalized with respect to the mean of the historical flow ensemble)

c

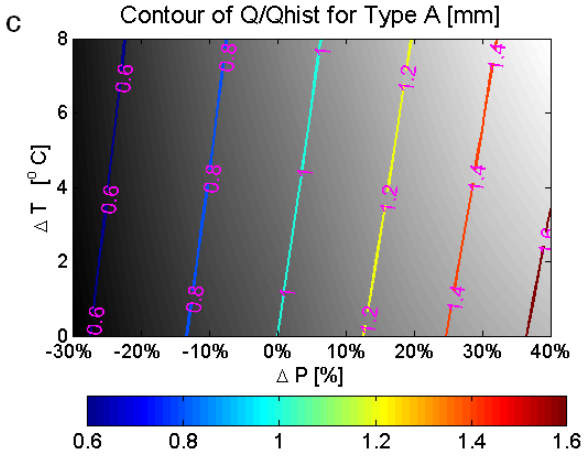
Contour of Q/Qhist for Type A [mm]
Δ T [^{0} C]
Δ P [%]
-30% -20% -10% 0% 10% 20% 30% 40%
0 2 4 6 8
0.6 0.8 1 1.2 1.4 1.6
Variation in Q/Qhist

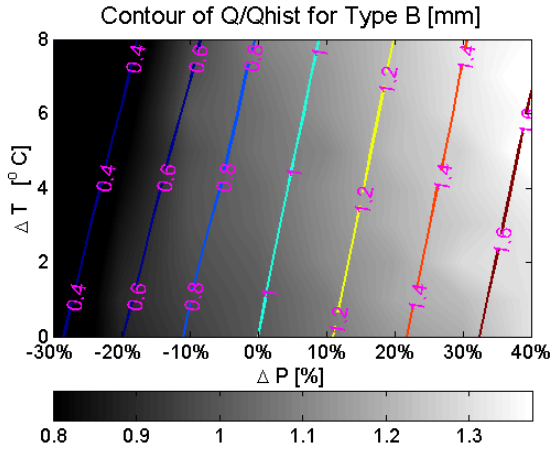
Contour of Q/Qhist for Type B [mm]
Δ T [^{0} C]
Δ P [%]
-30% -20% -10% 0% 10% 20% 30% 40%
0 2 4 6 8
0.8 0.9 1 1.1 1.2 1.3
Variation in width of the band (normalized with respect to the mean of the historical flow ensemble)

d

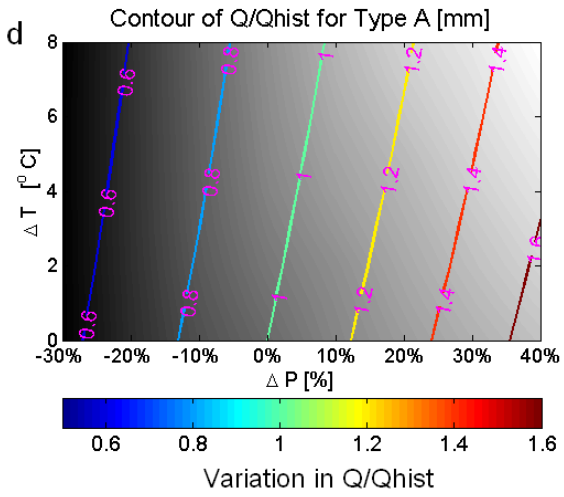

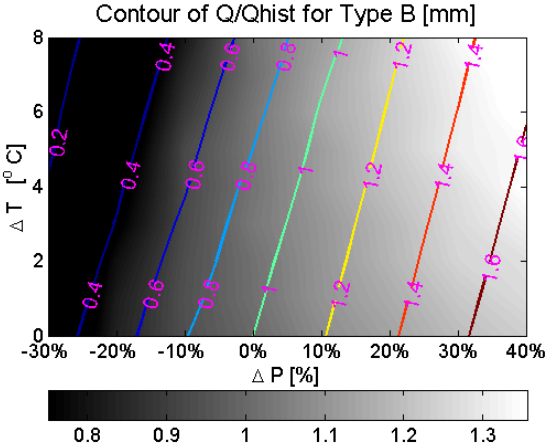

Variation in width of the band (normalized with respect to the mean of the historical flow ensemble)

e

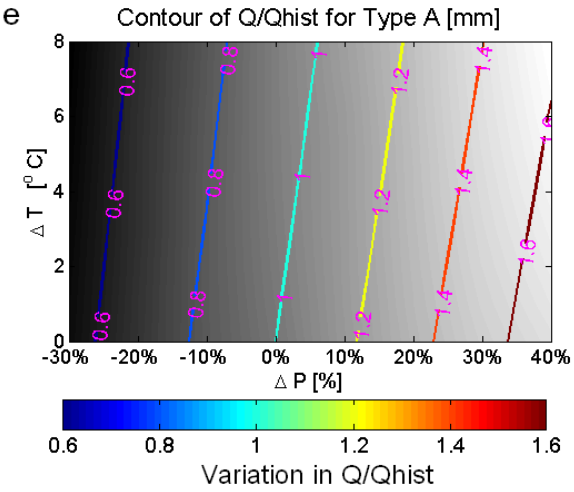

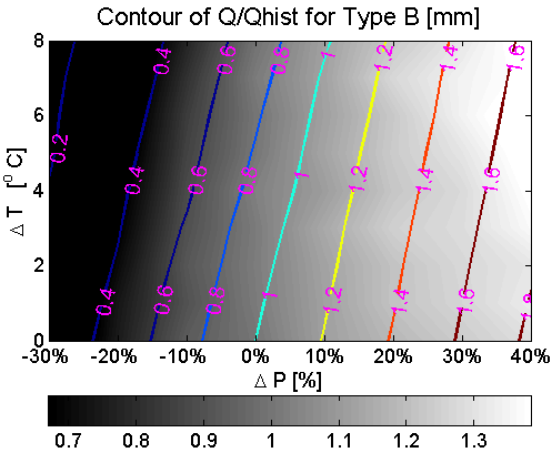

Variation in width of the band (normalized with respect to the mean of the historical flow ensemble)

f

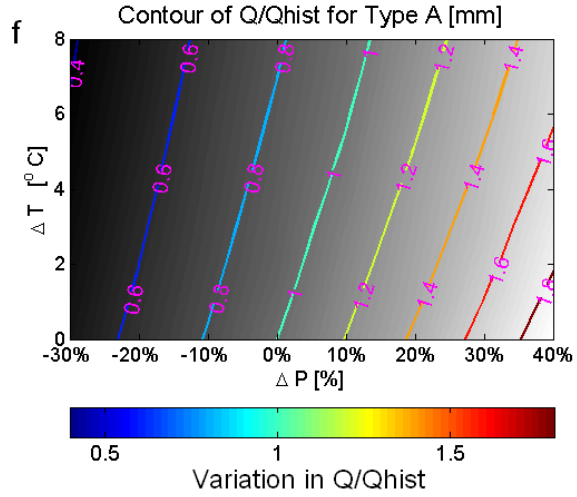

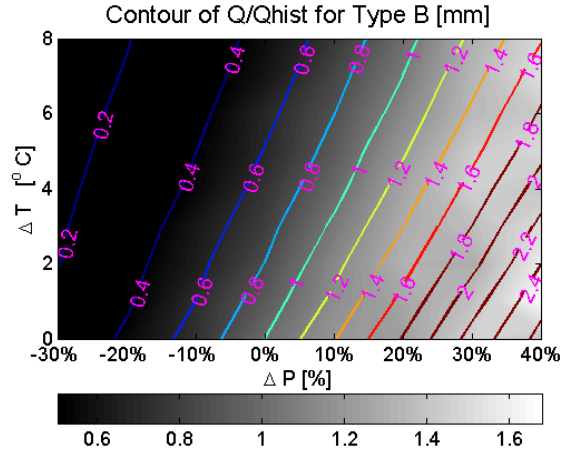

Variation in width of the band (normalized with respect to the mean of the historical flow ensemble)

Figure 5-6 (a-f). Contour plots of Q/Q_{hist} for mean of ensemble flow predictions for a given climate . Q_{hist} is the mean of the ensemble for no change in temperature or precipitation scenario). Q is the mean of the ensemble for the given climatic scenario. The background contours are normalized width of the band (Q_{max}-Q_{min}) for a given climate scenario normalized with respect to the width in the historical period (No change in temperature or precipitation scenario). The figures are ordered as: (a) Lower Androscoggin, (b) Lochsa, (c) Escambia, (d) Meramec, (e) Peace and (f) Yampa watersheds.

There are several key features of the contour plots in general, which we discuss before comparing them with respect to the Type A and Type B ensembles or across watersheds:

- The slope of the Q/Q_{hist} contours display the sensitivity to temperature/precipitation, the steeper the slope the lesser the sensitivity to temperature/precipitation and vice versa.
- The spacing between the contours also determines how extreme the change is. If the contours are spaced close together, it depicts that the change from one climatic regime to another is steeper, or in other words the sensitivity is more.

Observations and inferences

The slope of the contours is greater than 45° indicating that the stremflow predictions are more sensitive to precipitation changes than they are to temperature changes. However, the sensitivity to temperature is not negligible. The fact that the slope of the lines remains more or less the same except for Yampa watershed, implies that relative dependence of streamflow on temperature and precipitation does not change with climate. One of the possible reasons for a low temperature sensitivity can be that we are using a temperature change scale in °C and precipitation change scale in (%). If we use a similar percentage change in PE approach, the results might be different.

- The spacing between the contours is lesser for Type B ensembles, this implies that Type B constraints produce streamflow values that are more sensitive to temperature and precipitation than Type A constraints. This implies that Type B predictions display more sensitivity to

climate change than Type B predictions. This is due to the incorporation of Budyko curve to include the impact of climate on parameters.

- The width of the band for Type B constraints is always smaller in the drier period, than the Type A constraint. This is inferred from the extent of intrusion of black surface in the background for Type B constraints. This implies that the predicted range gets smaller for drier periods for Type B constraints, or the uncertainty in prediction decreases.
- The spacing for both Type A and Type B ensembles decreases as we move from watersheds with low aridity index to ones with a high aridity index. This implies that both Type A and Type B constraints produce streamflows which become increasingly sensitive to precipitation as we move to water limited watersheds.
- For Type A predictions, all the basins show equal sensitivity to dry and wet climates except Yampa which shows greater sensitivity to wet regimes.
- For Type B predictions, Lochsa, Escambia, Meramec, Peace and Yampa watersheds show more sensitivity to dry climates. The Lower Androscoggin watershed shows equal sensitivity to both dry and wet climates, and Yampa watershed displays more sensitivity to wet climates.
- From these observations, we conclude that Type B projections show more sensitivity to dry climates in general. *Schaake and Nemek* (1982) also predicted that arid climates have greater sensitivity to changing climate than humid ones. This is true for non snow catchments.
- The trend is different for snow catchments where the projections depend on the percentage of snow present in the catchment. If the snow percentage is small, the catchment is more sensitive in dry regimes, if the snow percentage is more, it is more sensitive in wet regimes.
- The contours suggest that for a precipitation increase from 0% to 15% the predicted flow is equal to the historical flow with increasing temperature (Note the contour of value 1). However, for precipitation changes on the drier side, the predicted flow is always low. This has already been discussed previously.
- The Yampa watershed is different from other watersheds as it shows greater sensitivity in wetter regimes than in drier regimes even though it has a high aridity index. The skewness in

sensitivity is more pronounced for Type B ensembles but it is also evident for Type A ensemble prediction. This is attributed to the high percentage of snow in this catchment, which makes its behavior unlike the other catchments (as discussed previously). *Weiss and Alcamo* [2010] found that the snow dominated basins in Europe show a high sensitivity to climate change due to changes in the snowmelt. This is similar to observations of high sensitivity of Yampa watershed. However, the Lower Androscoggin and Lochsa watersheds do not show such a high sensitivity. This can be due to the facts that they lie in the energy limited region (low aridity index) and their snow percentage is smaller than that of the Yampa watershed.

- The contour maps developed by *Risbey and Entekhabi* (1996) for the Sacremento river basin and found out that the temperature dependence of streamflow was very weak. The contour plots developed here also show that the temperature dependence of streamflow is less than its precipitation dependence. However, the dependence on temperature is greater than what was found in their study.

Change of Model Parameters with Climate

It was found that several parameters of the model were impacted by the changes in constraints. The most significant impact was observed on the storage of the model which is given by equation 3. The storage was calculated for each climatic scenario from each set of accepted parameter. Therefore a group of storage value was arrived at. For comparing the change in storage, the median of every ensemble was taken. Then the deviation in storage was calculated as the difference between the median of the climate change ensemble to the median of the historical ensemble. The results are plotted in figure 5-7 (a-f). These results show that the storage increases as the climate becomes drier and warmer and vice versa. This is consistent with the study by *Merz et al.* [2010] where they also find an increase in storage parameter with increasing temperatures. They attribute this increase to an increasing amount of evaporation from the basin which allows the soil storage to go high. In this study, we attribute this increase to both increases of temperature and

decreases of precipitation, the evaporation going high in either case. However, the intensity of change is greater in dry climates than in wet climates. The other parameters were also evaluated in a similar manner and it was found that the parameter Ks was the next parameter which showed a trend with climate. The two parameters of the snow module showed small trends were : degree day factor and base temperature for melting. These trends are observed only in snow watersheds. α, Kq and threshold temperature for ice formation remained insensitive to climate change for this particular model.

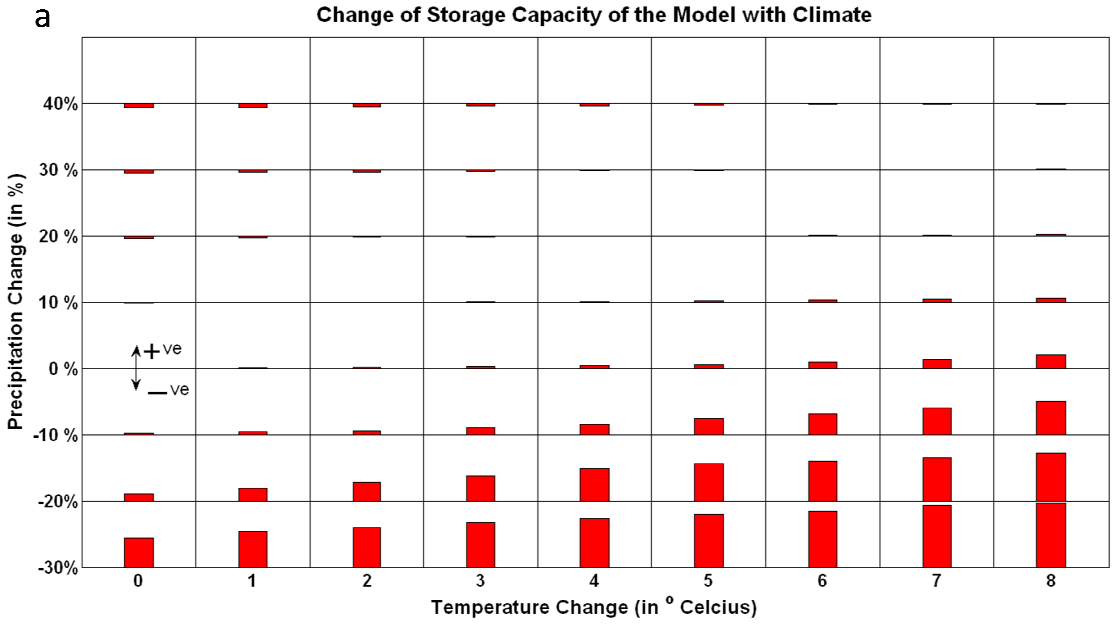

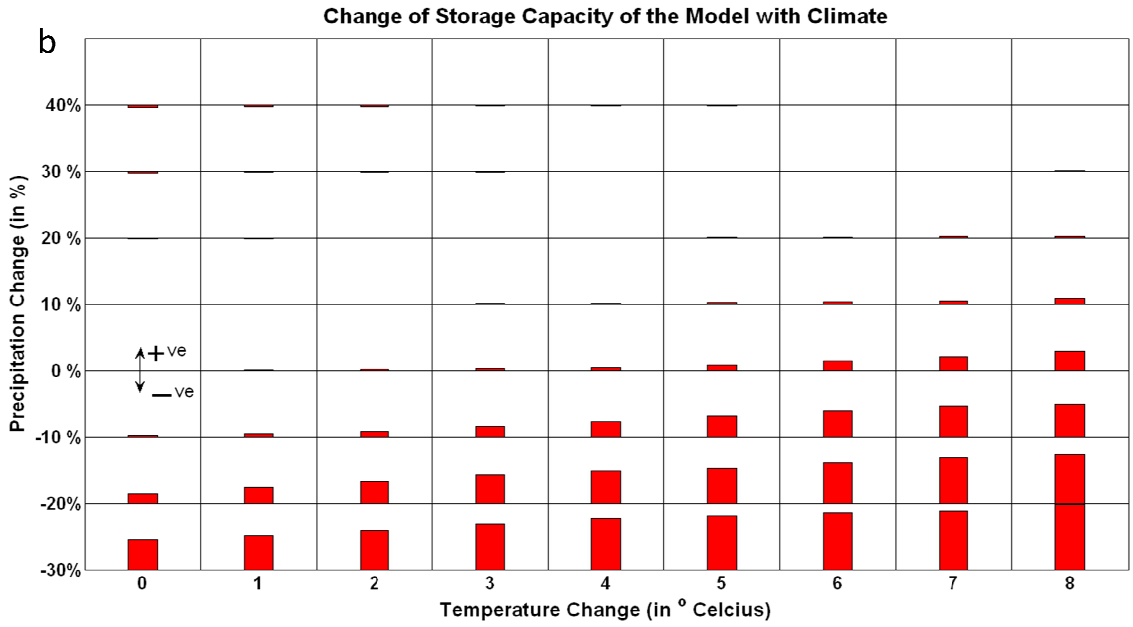

c

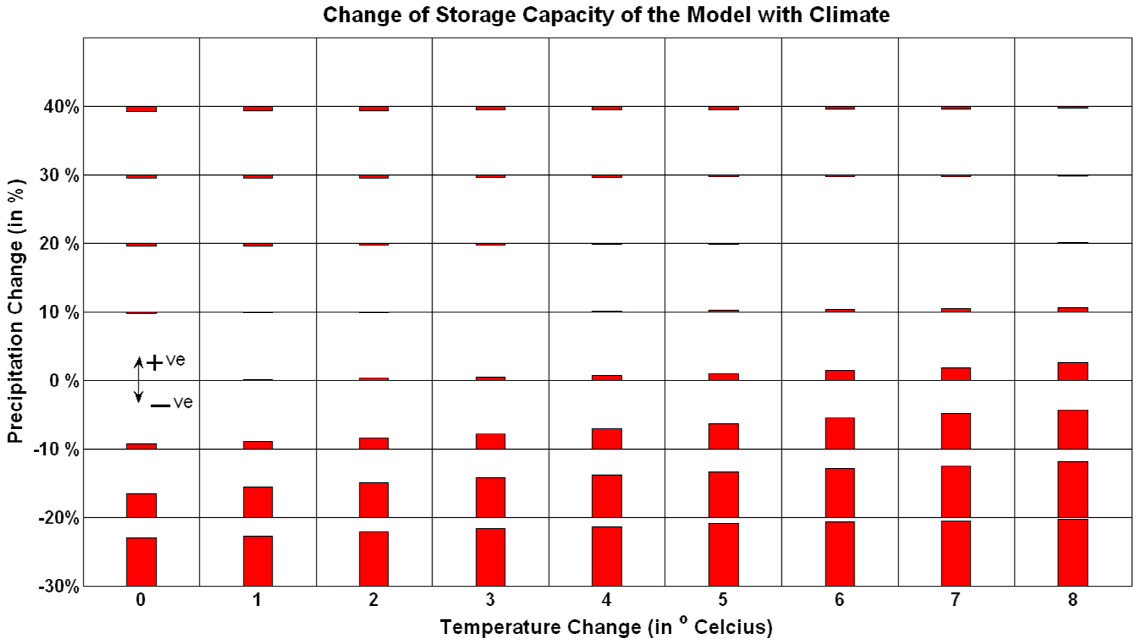
Change of Storage Capacity of the Model with Climate
Precipitation Change (in %)
40%
30 %
20 %
10 %
0 %
-10 %
-20%
-30%
+ve
-ve
0
1
2
3
4
5
6
7
8
Temperature Change (in ° Celcius)

d

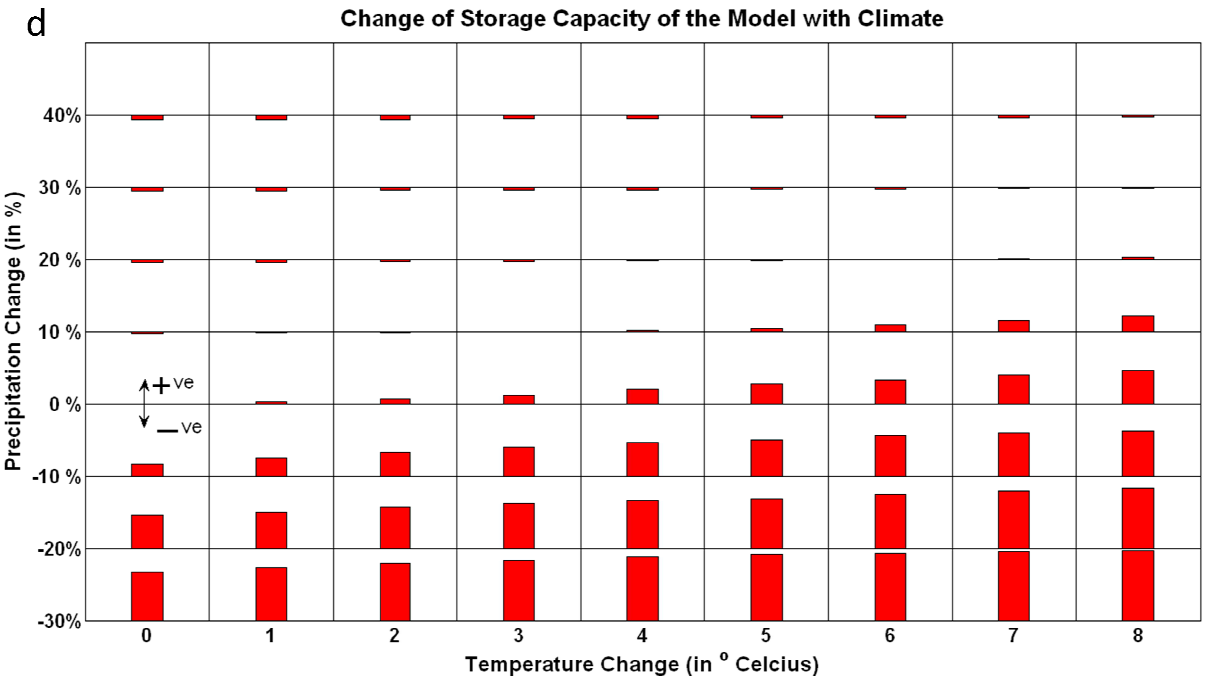
Change of Storage Capacity of the Model with Climate
Precipitation Change (in %)
40%
30 %
20 %
10 %
0 %
-10 %
-20%
-30%
+ve
-ve
0
1
2
3
4
5
6
7
8
Temperature Change (in ° Celcius)

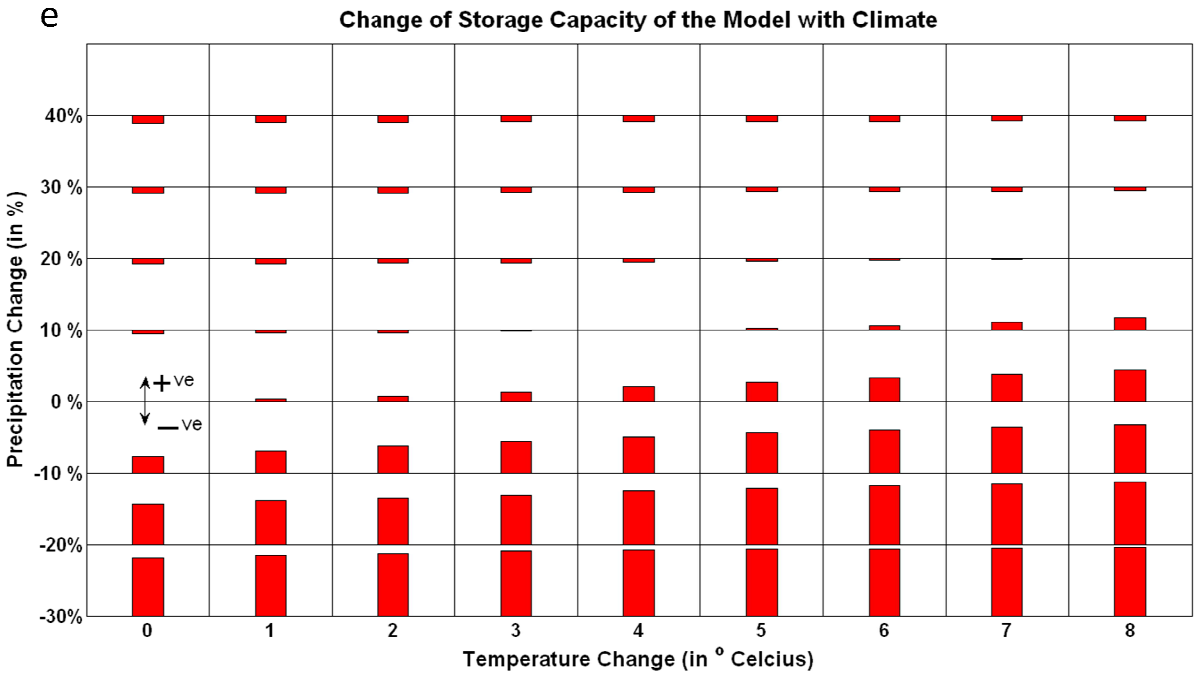

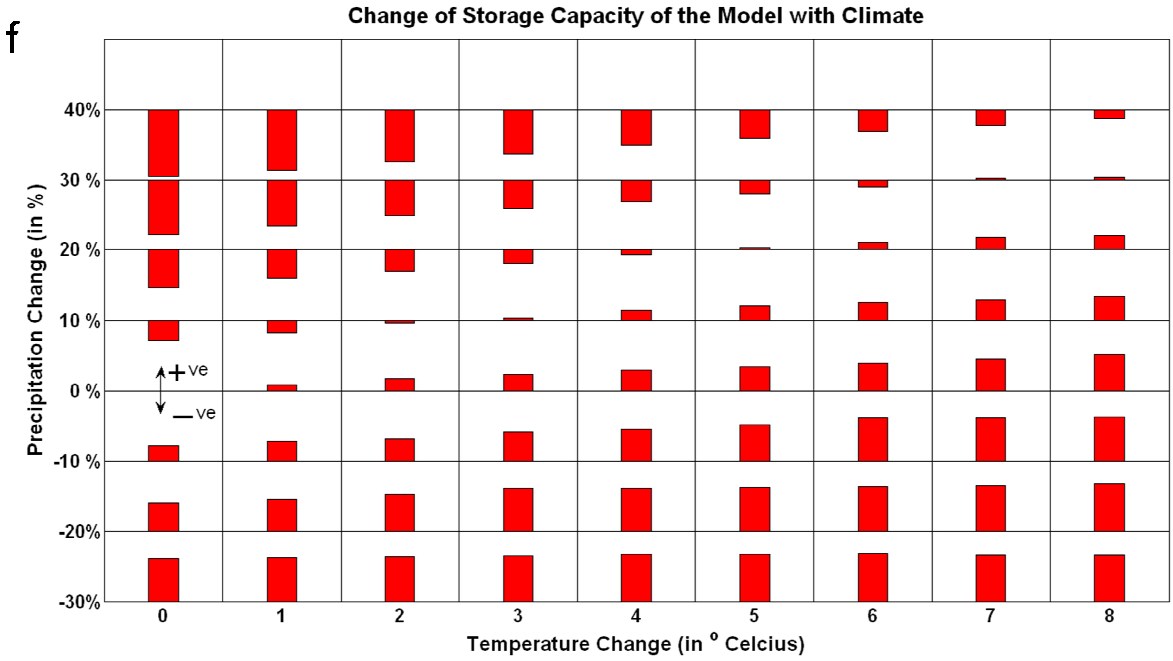

Figure 5-7 (a-f). Matrix of deviation from median of storage (calculated from cmax and b) values for study watersheds. The red boxes depict the deviation from the historical median of the storage. The figures are ordered as: (a) Lower Androscoggin, (b) Lochsa, (c) Escambia, (d) Meramec, (e) Peace and (f) Yampa watersheds.

Chapter 6

Conclusions

We provided a novel modeling framework for evaluating the impact of climate change on streamflow under the assumptions of nonstationarity of the climate and inclusive of uncertainty. The changes in behavioral model parameter ensembles expected to occur in a changing climate have been explicitly accounted for and the resultant matrices clearly show that under dry climates, the difference between the two approaches becomes significant. This is due to the manner in which watersheds shift along the Budyko curve. In dry climates, the PE/P is already high; a further increase in temperature increases the intensity of the impact. Also, noticeable was the behavior of watersheds in high temperature and high precipitation regimes. The similarity in model predictions that emerged from the similarity of constraints indicate that our assumptions of stationarity does not impact the predictions in such climates. Contour plots of elasticity provide useful information regarding the the differences and similarities between the two methodologies. Again, the position of the watershed on the Budyko curve along with its snow characteristics become the determining factors in the output. The analysis reinforces the fact that drier regimes are more sensitive to changes in temperature, an observation which is consistent with the analytical derivation in *Dooge* (1992) where he shows that the sensitivity factor approaches infinity as the aridity index approaches infinity. Similar observations are reported in *Vaze et. al* (2009) who state that prediction of runoff over dry periods by models calibrated on wet periods is worse than the prediction of runoff over wet periods by models calibrated over dry periods. The authors also discuss that after a certain change in mean precipitation, the performance of models with historical parameters break down. The study conducted here clearly shows why such a result should be expected.

We do not consider the change of other response characteristics with climate in this study, the main limitation being the regionalization of these characteristics. The outcome of the study depends on the model used as an increasingly complex model can model all processes and for an ideal model, the parameters will not change with time. There are other areas to explore in this study. One important aspect is the relationship between parameters and catchment characteristics. It can also be investigated whether the parameters filtered for the constraints used work well for other constraints that which were used for the process of filtereing. The most important question however is how different models, from conceptual to physical, behave in different climatic regime. All these issues will be taken up in the further research on this topic.

Nevertheless, for lumped conceptual models such as HyMod, we have developed a strategy to allow for such changes in the parameters. As was discussed, the impact of snow and position of the watershed on the budyko curve successfully explain most of the trend in the results. The change of storage in the watershed observed as a function of climate is another interesting result which bears implications for conceptual models being used for climate change studies. An important point is that this framework is applicable to both gauged and ungauged basins. We can either derive constraints from historical variability or through regionalization. It can therefore be applied to look at climate change impacts in less developed, and therefore usually less monitored, parts of the world. It also enables the testing of model behavior outside the range of historical variability, since the spatial gradients available can be much larger. We can now go beyond our historical observations and predict streamflow for climates that the watershed did not experience before. It also eliminates the need to correlate the parameter with catchment characteristics. Considering that we identified that increases in temperature combined with decreases in precipitation cause the most severe differences between traditional and our approach, it seems that current strategies underestimate the negative impact of climate change especially in warm/dry countries (many

of which are less developed). This suggests that the results of this study are most important for the most vulnerable parts of the world.

References

Boyle, D.P., Gupta, H.V. and Sorooshian, S., 2000. Towards improved calibration of hydrologic models: Combining the strengths of manual and automatic methods, *Water Resour. Res.*, **36**, 3663-3674.

Buytaert, W. and K. Beven (2009), Regionalization as a learning process, *Water Resour. Res.,* 45, W11419, doi:10.1029/2008WR007359.

Buytaert, W., R. Célleri, and L. Timbe (2009), Predicting climate change impacts on water resources in the tropical Andes: Effects of GCM uncertainty, *Geophys. Res. Lett.,* 36, L07406, doi:10.1029/2008GL037048.

Chiew, F. H. S., J. Teng, J. Vaze, D. A. Post, J. M. Perraud, D. G. C. Kirono, and N. R. Viney (2009), Estimating climate change impact on runoff across southeast Australia: Method, results, and implications of the modeling method, *Water Resour. Res.*, *45*, W10414, doi:10.1029/2008WR007338.

Christensen, J.H., B. Hewitson, A. Busuioc, A. Chen, X. Gao, I. Held, R. Jones, R.K. Kolli, W.-T. Kwon, R. Laprise, V. Magaña Rueda, L. Mearns, C.G. Menéndez, J. Räisänen, A. Rinke, A. Sarr and P. Whetton, (2007), Regional Climate Projections. In: *Climate Change 2007: The Physical Science Basis. Contribution of Working Group I to the Fourth Assessment Report of the Intergovernmental Panel on Climate Change* [Solomon, S., D. Qin, M. Manning, Z. Chen, M. Marquis, K.B. Averyt, M. Tignor and H.L. Miller (eds.)]. Cambridge University Press, Cambridge, United Kingdom and New York, NY, USA

Clark, M. P. and J. A. Vrugt (2006), Unraveling uncertainties in hydrologic model calibration: Addressing the problem of compensatory parameters, *Geophys. Res. Lett.*, *33*, L06406, doi:10.1029/2005GL025604.

Dewalle D.R. and A. Rango (2008), *Principles of Snow Hydrology*, Cambridge University Press, Cambridge, UK.

Dooge, J., 1992: Sensitivity of runoff to climate change: A Hortonian approach. *Bull. Amer. Meteor. Soc*., 73, 2013-2024.

Dooge, J. C. I., M. Bruen, and B. Parmentier (1999), A simple model for estimating the sensitivity of runoff to long-term changes in precipitation without a change in vegetation, *Adv. Water Resour.*, 23, 153 – 163.

Fu, G., S. P. Charles, and F. H. S. Chiew (2007), A two-parameter climate elasticity of streamflow index to assess climate change effects on annual streamflow, *Water Resour. Res.*, *43*, W11419, doi:10.1029/2007WR005890.

Ghosh, S. and P. P. Mujumdar (2009), Climate change impact assessment: Uncertainty modeling with imprecise probability, *J. Geophys. Res.*, *114*, D18113, doi:10.1029/2008JD011648.

Hay L. E., G. J. McCabe (2010), Hydrologic effects of climate change in the Yukon River Basin, *Climatic Change*, 100:509–523, DOI 10.1007/s10584-010-9805-x

Hundecha, Y. und A. Bárdossy (2004), Modeling of the effect of land use changes on the runoff generation of a river basin through parameter regionalization of a watershed model, *J. Hydrology*,292 281-295.

Hundecha, Y., T. B. M. J. Ouarda, and A. Bárdossy (2008), Regional estimation of parameters of a rainfall-runoff model at ungauged watersheds using the “spatial” structures of the parameters within a canonical physiographic-climatic space, *Water Resour. Res.*, *44*, W01427, doi:10.1029/2006WR005439.

Jha, M., Z. Pan, E. S. Takle, and R. Gu (2004), Impacts of climate change on streamflow in the Upper Mississippi River Basin: A regional climate model perspective, *J. Geophys. Res.*, *109*, D09105, doi:10.1029/2003JD003686.

Jiang, T., Y.D. Chen, X. Chong-yu, X. Chen, X. Chen, and V.P. Singh (2007). Comparison of hydrological impacts of climate change simulated by six hydrological models in the Dongjiang Basin, South China. *J. Hydrology, 336, 316– 333*

Jones R. N., H.S. C. Francis, W.C. Boughton, and L. Zhang (2006), Estimating the sensitivity of mean annual runoff to climate change using selected hydrological models, *Adv. Water Resour.* (29), 1419-1429, doi:10.1016/j.advwatres.2005.11.001

Khadam, I. M. and J. J. Kaluarachchi (2004), Use of soft information to describe the relative uncertainty of calibration data in hydrologic models, *Water Resour. Res.*, *40*, W11505, doi:10.1029/2003WR002939.

Knowles, N., and D. R. Cayan (2002), Potential effects of global warming on the Sacramento/San Joaquin watershed and the San Francisco estuary, *Geophys. Res. Lett.*, 29(18), 1891, doi:10.1029/2001GL014339.

Kundzewicz, Z. W., L. J. Mata, N. W. Arnell, P. Doll, B. Jimenez, K. Miller, T. Oki, Z. Sen and I. Shiklomanov (2008). The implications of projected climate change for freshwater resources and their management. *Hydrological Sci. J.*, *53*(1), 3-10.

Legesse D., T. A. Abiye , and C. Vallet-Coulomb (2010), Modeling impacts of climate and land use changes on watershed hydrology: Meki River, Ethiopia, *Hydrol. Earth Syst. Sci. Discuss.*, doi:10.5194/hessd-7-4535-2010

Maidment, D.R. (1993*), Handbook of Hydrology*, Mc Graw-Hill, Inc.

Maurer, E. P., and P. B. Duffy (2005), Uncertainty in projections of streamflow changes due to climate change in California, *Geophys. Res. Lett.,* 32, L03704, doi:10.1029/2004GL021462.

Merz R., J. Parajka, and G. Blöschl (2010), Time Stability of watershed model parameters – implications for climate impact analyses. *Water Resour. Res.,* doi:10.1029/2010WR009505, in press.

Milly, P. C. D., K. A. Dunne and A. V. Vecchia (2005). Global pattern of trends in streamflow and water availability in a changing climate. *Nature*, *438*(7066), 347-350.

Milly, P. C. D., R. T. Wetherald, K. A. Dunne and T. L. Delworth (2002). Increasing risk of great floods in a changing climate. *Nature*, *415*(6871), 514-517.

Moore, R. J. (2007). The PDM rainfall-runoff model. *Hydrol. Earth Syst. Sci.*, *11*(1), 483-499.

Nash, L. L., and P. H. Gleick (1991) Sensitivity of streamflow in the Colorado basin to climatic changes, *J. Hydrol.*, 125, 221–241.

Nemec J. and J. Schaake (1982). Sensitivity of water resources systems to climate variation. *Hydrological Sci. J.*, 27(3),

Nohara, D., A. Kitoh, M. Hosaka and T. Oki (2006). Impact of climate change on river discharge projected by multimodel ensemble. *J. Hydrometeorol.*, *7*(5), 1076-1089.

Pike, J.G. (1964). The estimation of annual runoff from meteorological data in tropical climate. *J. Hydrology*, 2, 116-123.

Risbey, J. S., and D. Entekhabi (1996), Observed Sacramento Basin stream-flow response to precipitation and temperature changes and its relevance to climate impacts studies*, J. Hydrol.*, 184, 209 – 223.

Rosero, E., Yang, Z.-L., Wagener, T., Gulden, L.E., Yatheendradas, S., and Niu, G.-Y. (2010), Quantifying parameter sensitivity, interaction and transferability in hydrologically enhanced versions of the Noah-LSM over transition zones during the warm season, *J. Geophys. Res.*, 115, D03106, doi:10.1029/2009JD012035

Santhi C., P.M. Allen, R.S. Muttiah, J.G. Arnold, and P. Tuppad (2008), Regional estimation of base flow for the conterminous United States by hydrologic landscape regions, *J. Hydrol.*, 351, 139-153, doi:10.1016/j.jhydrol.2007.12.018

Sankarasubramanian, A., R. M. Vogel, and J. F. Limbrunner (2001), Climate elasticity of streamflow in the United States, *Water Resour. Res.*, *37*(6), 1771–1781, doi:10.1029/2000WR900330.

Schaake J.C. and C. Liu (1989). Development and application of simple water balance models to understand the relationship between climate and water resources, *New*

Directions for Surface Water Modelin.:343-352, IAHS Publication, N 181. Wallingford.

Van Werkhoven, K., Wagener, T., Reed, P. and Tang, Y (2008). Characterization of watershed model behavior across a hydroclimatic gradient. *Water Resour. Res.,* 44. doi:10.1029/2007WR006271

Vaze J., D.A. Post, F.H.S Chiew, J-M Perraud, N.R. Viney, J. Teng (2010). Climate nonstationarity – Validity of calibrated rainfall-runoff models for use in climate change studies, *J. Hydrol.,*394, 447-457, doi:10.1016/j.jhydrol.2010.09.018

Vogel, R. M., I. Wilson, and C. Daly (1999), Regional regression models of annual streamflow for the United States, *J. Irrig. Drain. Eng.*, 125, 148 – 157.

Wagener, T., M. Sivapalan, P. A. Troch, B. L. McGlynn, C. J. Harman, H. V. Gupta, P. Kumar, P. S. C. Rao, N. B. Basu, and J. S. Wilson (2010), The future of hydrology: An evolving science for a changing world, *Water Resour. Res.,* 46, W05301, doi:10.1029/2009WR008906.

Wagener, T., Boyle, D.P., Lees, M.J., Wheater, H.S., Gupta, H.V. and Sorooshian, S. 2001. A framework for development and application of hydrological models. *Hydrol. Earth Syst. Sci.*, 5(1), 13-26.

Wagener, T. 2007. Can we model the hydrologic implications of environmental change? *J. Hydrol.*, 21(23), 3233-3236.

Weiss, M., and J. Alcamo (2010), A systematic approach to assessing the sensitivity and vulnerability of water availability to climate change in Europe, *Water Resour. Res.,* doi:10.1029/2009WR008516, in press.

Wood, A. W., L. R. Leung, V. Sridhar, and D. P. Lettenmaier (2004), Hydrologic implications of dynamical and statistical approaches to downscaling climate model outputs, *Climatic Change* 62: 189–216.

Yadav, M., T. Wagener and H. Gupta (2007), Regionalization of constraints on expected watershed response behavior for improved predictions in ungauged basins, *Adv. Water Resour.*(30), 1756-1774, doi:10.1016/j.advwatres.2007.01.005.

Zhang, Z., T. Wagener, P. Reed, and R. Bushan (2008), Ensemble streamflow predictions in ungauged basins combining hydrologic indices regionalization and multiobjective optimization, *Water Resour. Res.,* 44, W00B04. doi:10.1029/2008WR006833

Zheng, H., L. Zhang, R. Zhu, C. Liu, Y. Sato, and Y. Fukushima (2009), Responses of streamflow to climate and land surface change in the headwaters of the Yellow River Basin, *Water Resour. Res.*, *45*, W00A19, doi:10.1029/2007WR006665.

Appendix A

Parameter	Lower Limit	Upper Limit
Cmax * - maximum height of soil moisture store [mm]	0	800
b*- probability distribution factor [-]	0	5
α* - distribution factor for slow and quick flow [-]	0	1
K_q* - time constant for quick flow [day]	1	14
K_s* - time constant for slow flow [day]	14	300
D* - degree day factor [mm/day/°C]	0	20
T_b* - base temperature for melting [°C]	-5	5
T_t* - threshold temperature for snow formation [°C]	-5	5

Table A-1 Description and ranges of model parameters.

Name of Watershed	Daily NSE	Monthly NSE
Lower Androscoggin	0.7079	0.8685
Lochsa	0.8703	0.9285
Escambia	0.7252	0.8508
Meramec	0.5365	0.8086
Yampa	0.7063	0.8003
Peace	0.7051	0.8279

Table A-2. Best NSE (Nash-Sutcliffe) performance of case study watersheds (optimal value is 1). The NSE is the best among the set of 10000 NSEs calculated from the 10000-parameter sets considered in this study.

Appendix B

Selection of Constraints

For each constraint considered, 10,000 parameter sets were generated and a separation into behavioral and non-behavioral was performed in the following manner:

- The upper and lower limits of new constraints were evaluated by adding and subtracting a certain percentage of the historical average value of the constraint. These limits were then used for filtering behavioral parameter sets from the generated 10,000 parameter sets.
- Both reliability and sharpness are defined according to *Yadav et al.*, [2007]. Reliability is defined as the measure of the fraction of time the observed streamflw ois within the prediction band of the model. The greater the reliability the better the performance of the constraint. Sharpness is a measure of the ensemble spread, a single line having a sharpness of 100% and the original ensemble having a sharpness of 0%. The higher the sharpness the better the constraining capacity.
- The first year of simulation was removed while calculating reliability and sharpness to account for warm up period.
- From the filtered parameter sets, the upper bound and lower streamflow values corresponding to each percentage were plotted.

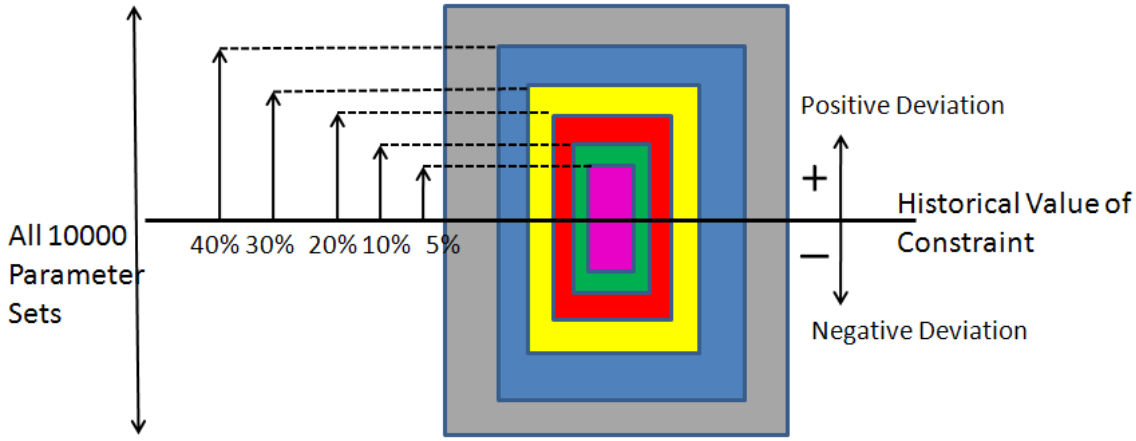

Figure B-1. Description of methodology adopted for evaluating the effectiveness of constraint. The deviation is from the historical value of given constraint and the limits are ±5%,±10%, ±20%, ±30% and ±40 % of the historical value. These limits are used for the filtering acceptable parameter sets from the ensemble of 10000 parameter sets.

Performance of ROC-BFI as constraint

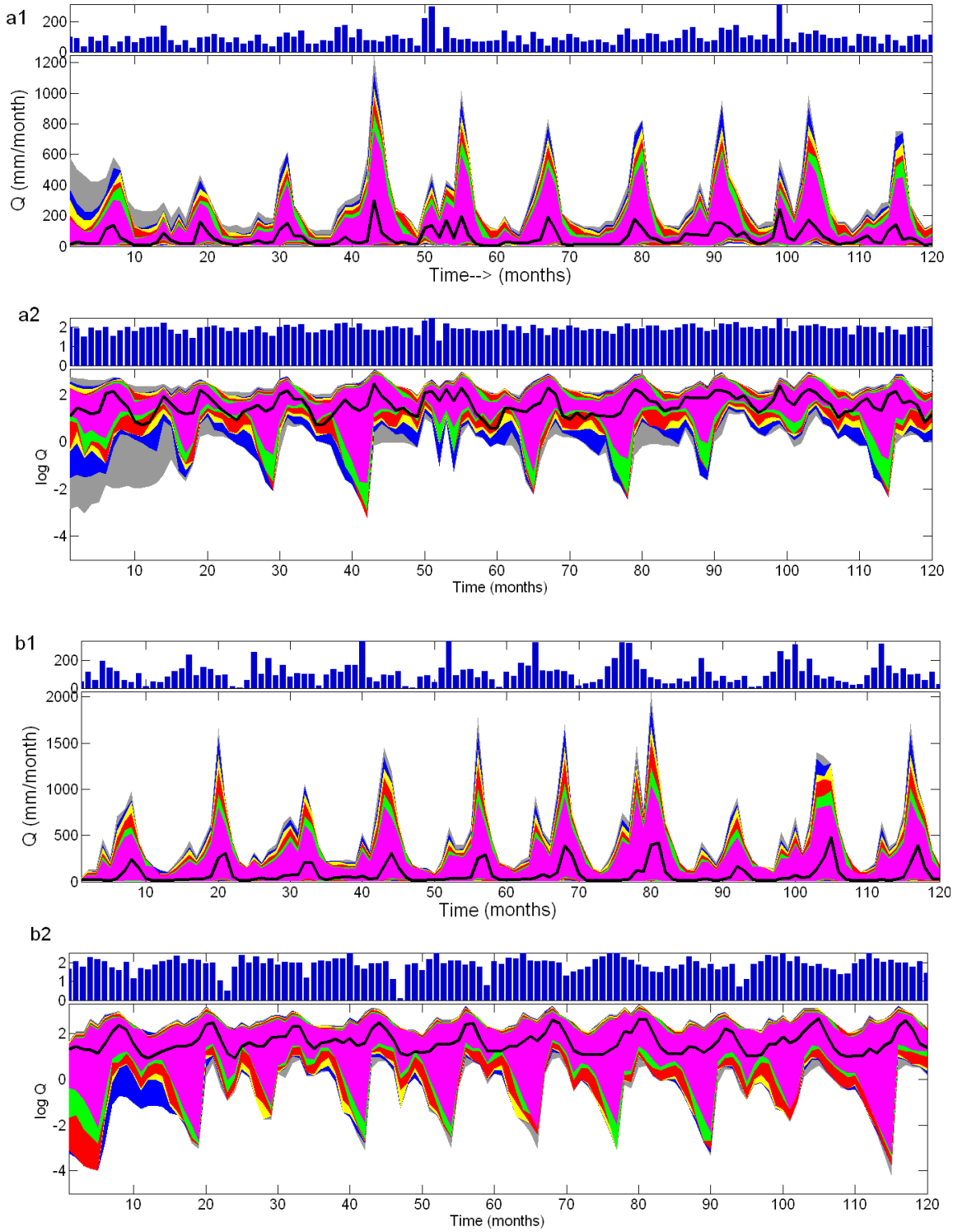

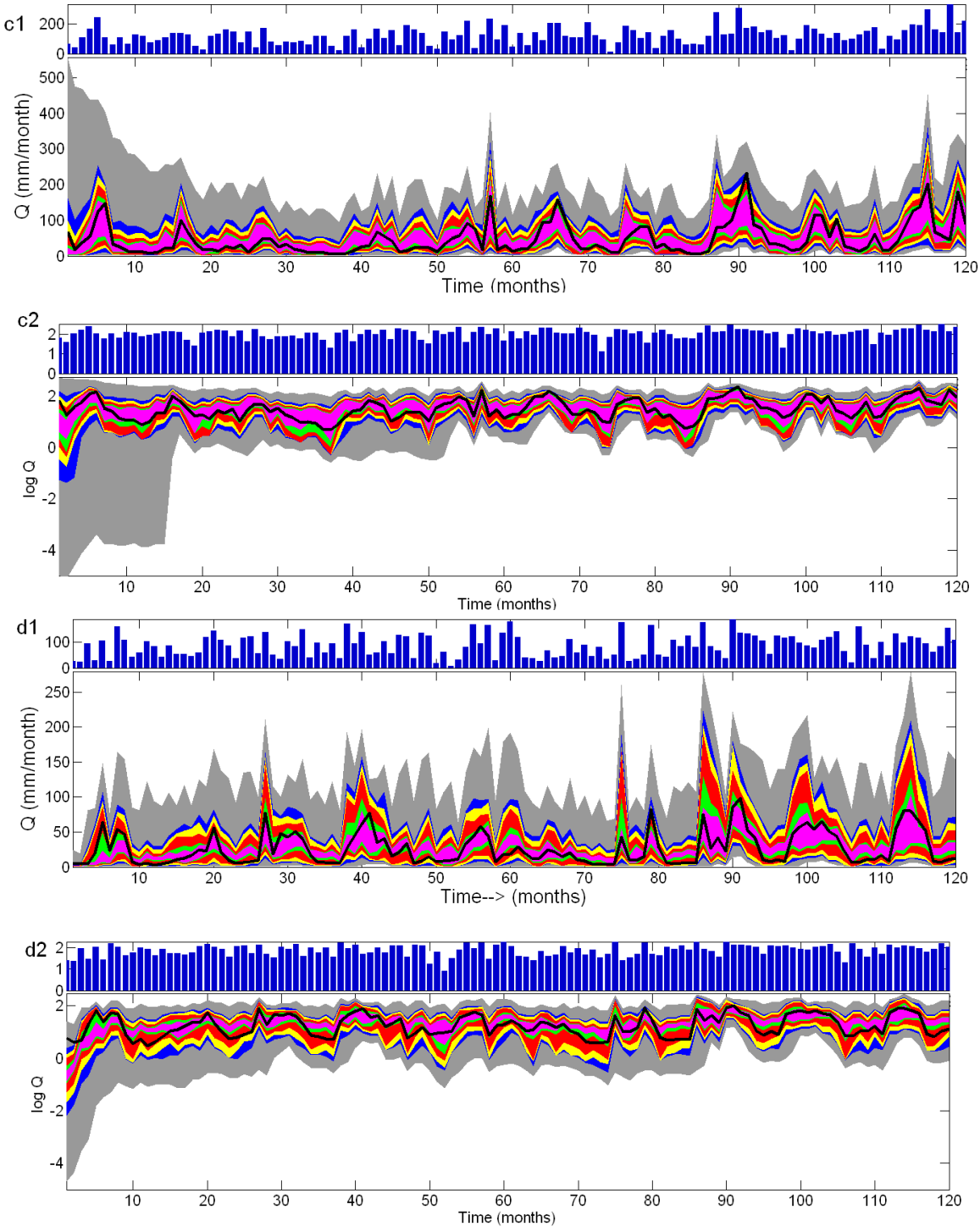
c1
Q (mm/month)
Time (months)
c2
log Q
Time (months)
d1
Q (mm/month)
Time--> (months)
d2
log Q
Time (months)

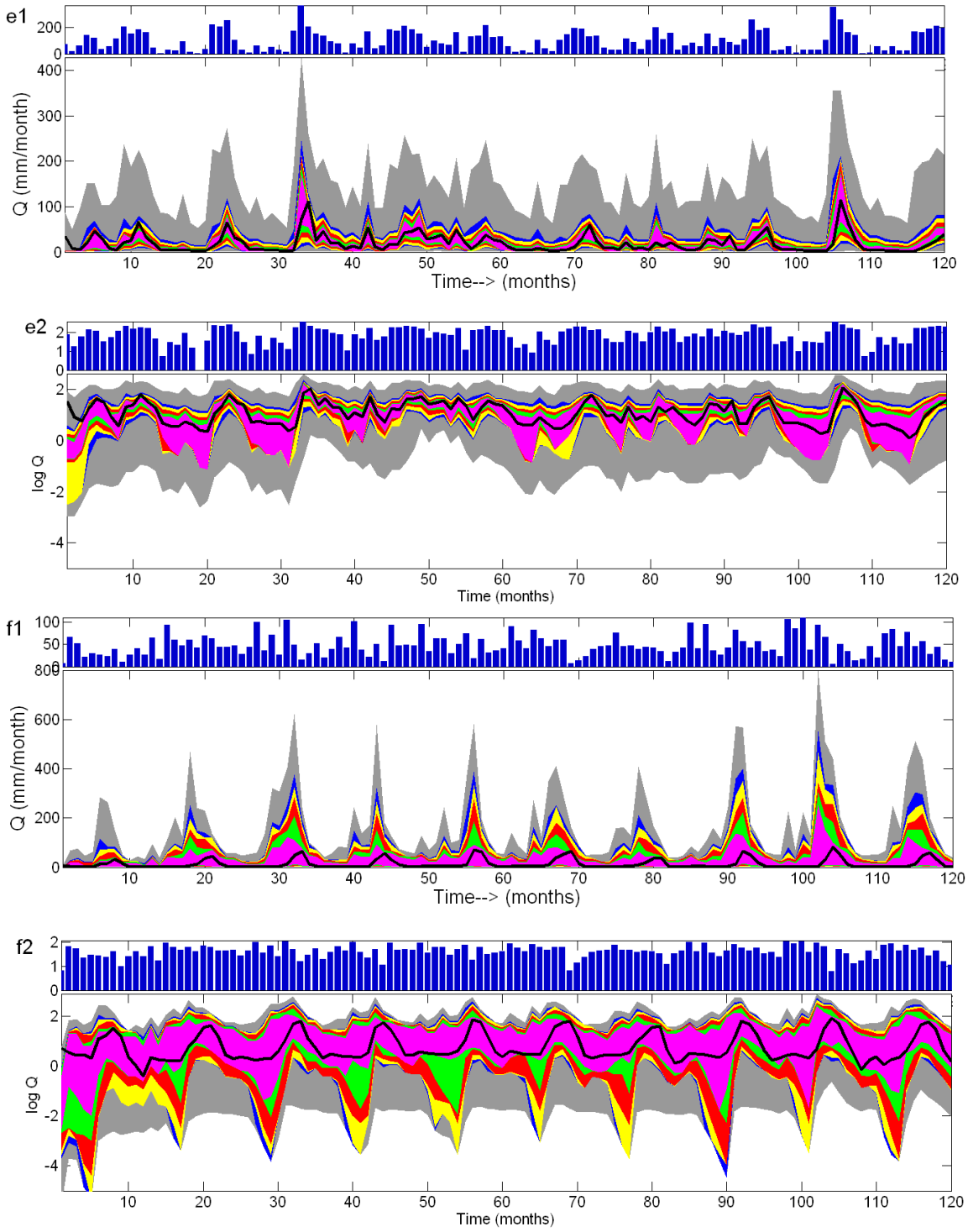

Figure B-2. Performance of combination of runoff ratio and Baseflow index for watersheds, in order: (a) Lower Androscoggin, (b) Lochsa, (c) Escambia, (d) Meramec, (e) Peace and (f) Yampa watersheds.

ROC-BFI	#1	#2	#3	#4	#5	#6
Total	1.00	1.00	1.00	1.00	1.00	1.00
5%	0.78	0.97	0.43	0.94	0.73	0.86
10%	0.84	1.00	0.63	1.00	0.85	0.92
20%	1.00	1.00	0.97	1.00	0.98	0.98
30%	1.00	1.00	1.00	1.00	0.99	1.00
40%	1.00	1.00	1.00	1.00	1.00	1.00

Table B-1. Reliability Estimates of the 6 Watersheds under the ROC-BFI constraint in order: (1) Lower Androscoggin, (2) Lochsa, (3) Escambia, (4) Meramec, (5) Peace and (6) Yampa watersheds.

ROC-BFI	#1	#2	#3	#4	#5	#6
Total	0.00	0.00	0.00	0.00	0.00	0.00
5%	48.48	33.73	79.18	63.59	70.67	81.17
10%	37.00	26.05	73.31	55.60	65.39	77.41
20%	23.30	15.85	59.19	45.27	55.89	72.70
30%	15.49	9.45	50.68	37.18	48.53	67.34
40%	10.22	5.25	44.15	31.93	40.63	62.12

Table B-2. Sharpness Estimates of the 6 Watersheds under the ROC-BFI constraint in order: (1) Lower Androscoggin, (2) Lochsa, (3) Escambia, (4) Meramec, (5) Peace and (6) Yampa watersheds

ROC-BFI	#1	#2	#3	#4	#5	#6
Total	0.00	0.00	0.00	0.00	0.00	0.00
5%	53.71	34.15	79.20	61.73	69.79	71.03
10%	42.36	26.30	73.14	53.10	63.15	67.05
20%	28.79	11.68	55.65	39.10	49.57	61.46
30%	22.04	7.45	44.43	32.28	42.45	55.00
40%	9.91	4.00	36.75	29.80	34.54	51.42

Table B-3. Sharpness Estimates of the 6 Watersheds for log transformed flow values under the ROC-BFI constraint in order: (1) Lower Androscoggin, (2) Lochsa, (3) Escambia, (4) Meramec, (5) Peace and (6) Yampa watersheds

Appendix C

Regionalization of Runoff Ratio

394 Watersheds were finally chosen to regionalize runoff ratio. Three equations were used to regress the aridity index with the runoff ratio (Dooge, 1992):

- Schreiber
- Ol'dekop
- Turc-Pike

The Schreiber fit was found to be the best since it remained below the AE=PE line all the time unlike others in which the confidence or prediction intervals crossed the AE=PE line. The resulting plots show 90% confidence and prediction limits as well as the fitted curve. The plot for Schreiber is shown in the main text of the thesis.

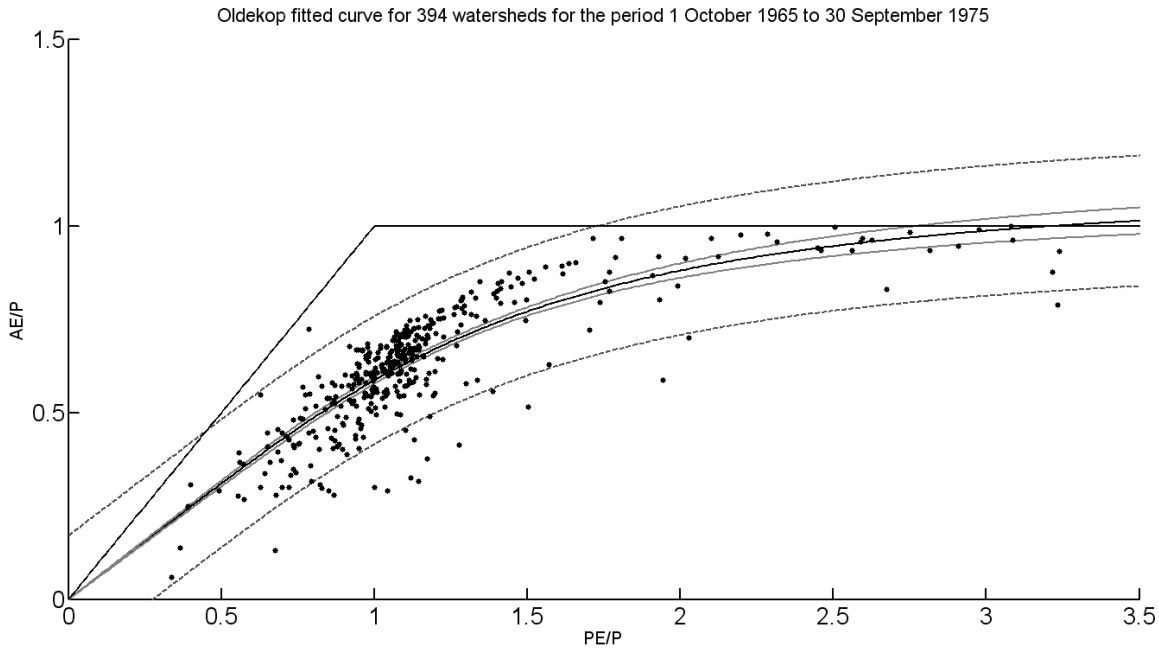

Figure C-1. Regionalized relationship for Oldekop Equation across 394 watersheds for the period 1 October 1065 to 30 September 1975

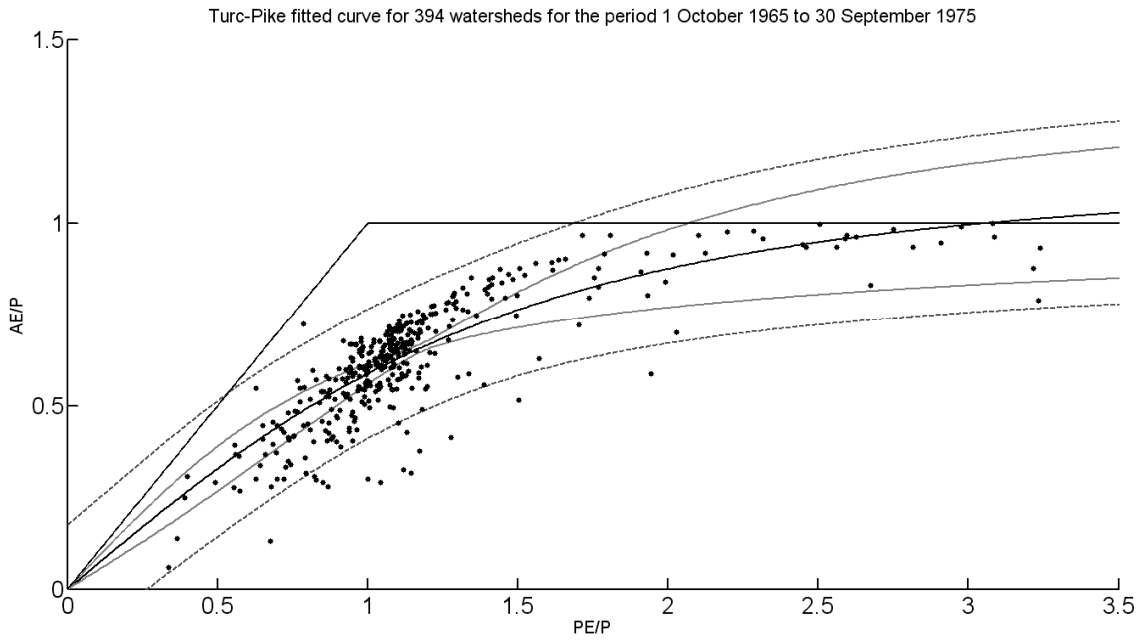

Figure C-2. Regionalized relationship for Turc-Pike Equation across 394 watersheds for the period 1 October 1065 to 30 September 1975

Appendix D

Regionalization of Baseflow Index:

Determination of Range for the baseflow index

The base flow index used throughout the study is a 3 pass filter base flow index value as suggested by by *Santhi et a.* (2008). In the following figure, we plot the histogram of the base flow index of 6 watersheds, with a fitted normal distribution. The ±1, ±2 and ±3 standard deviations are also plotted. Finally the standard deviation that covers the base flow index best is ±2 Std. for all watersheds and it is this value that was chosen as a constraint based on the historical data. It is to be noted that the assumption is that the BFI does not change with climate, since climate does not appear in the range of variables used for regionalization of BFI within our dataset.

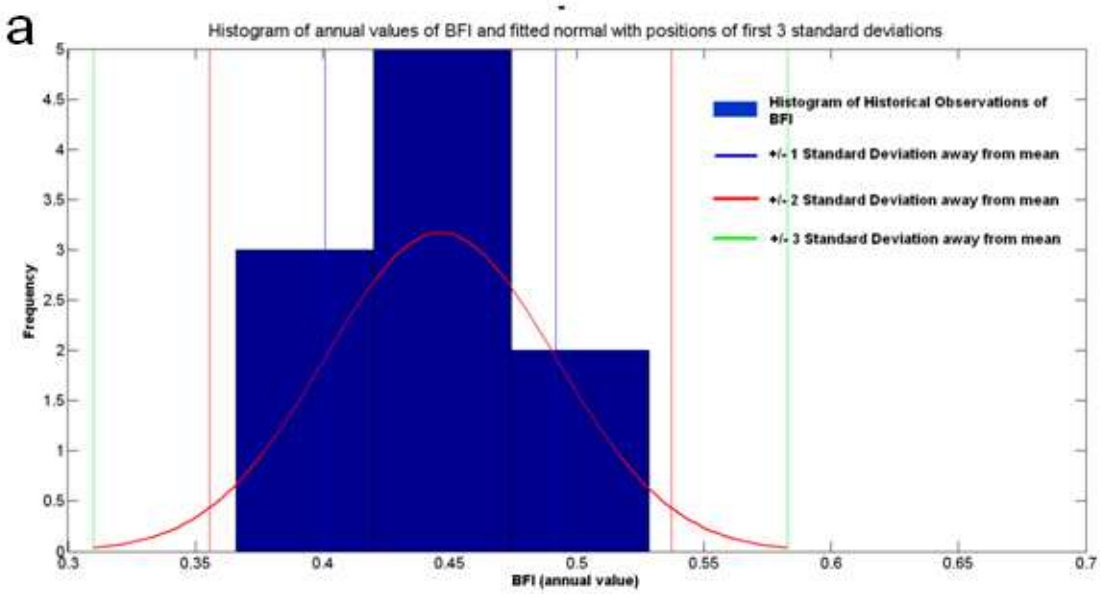

b

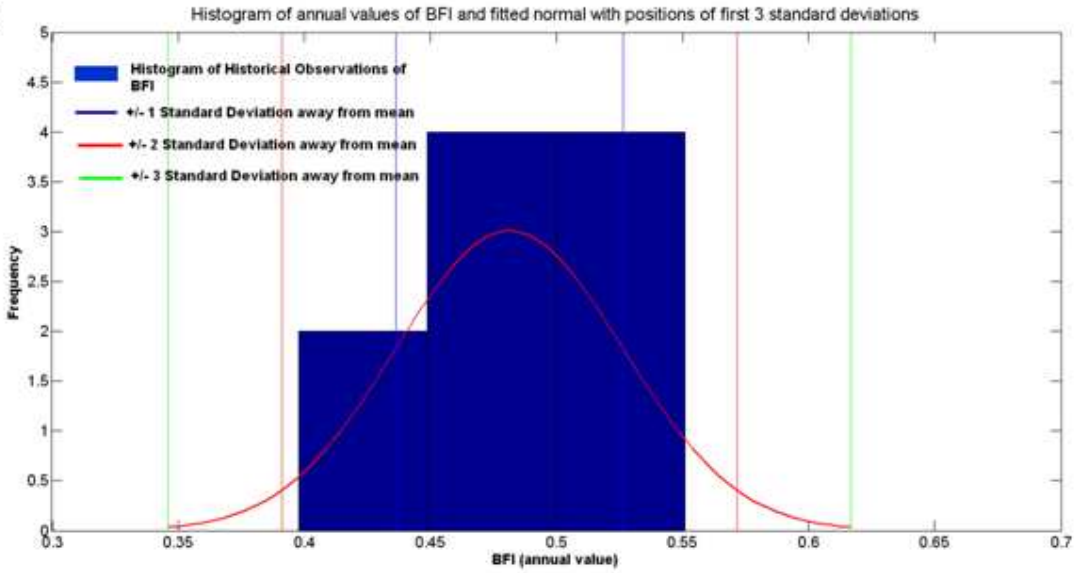
Histogram of annual values of BFI and fitted normal with positions of first 3 standard deviations
Histogram of Historical Observations of BFI
+/- 1 Standard Deviation away from mean
+/- 2 Standard Deviation away from mean
+/- 3 Standard Deviation away from mean
Frequency
BFI (annual value)

c

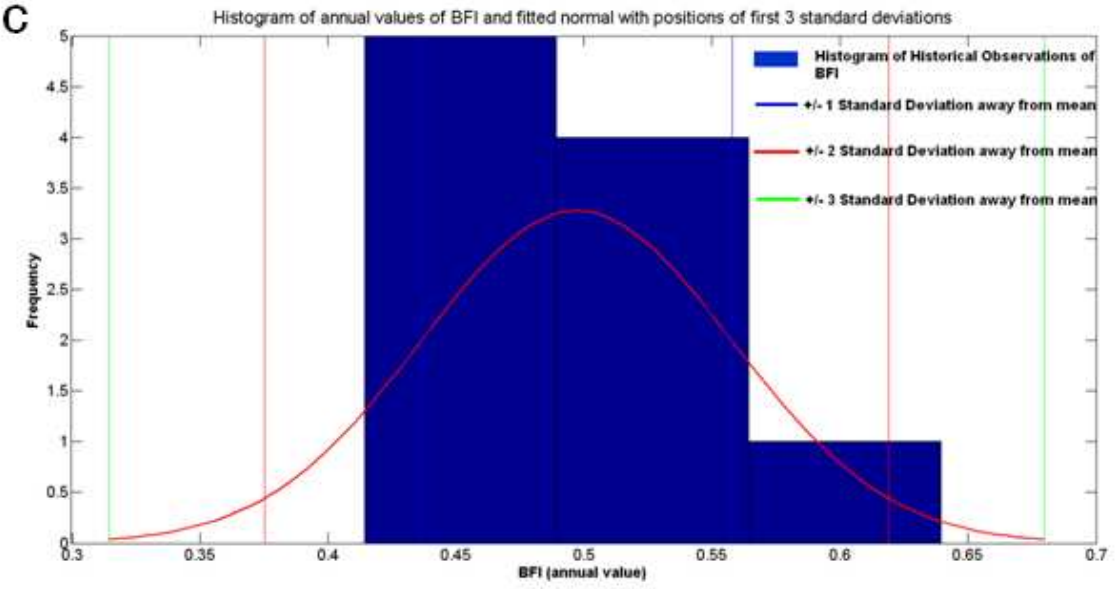
Histogram of annual values of BFI and fitted normal with positions of first 3 standard deviations
Histogram of Historical Observations of BFI
+/- 1 Standard Deviation away from mean
+/- 2 Standard Deviation away from mean
+/- 3 Standard Deviation away from mean
Frequency
BFI (annual value)

d

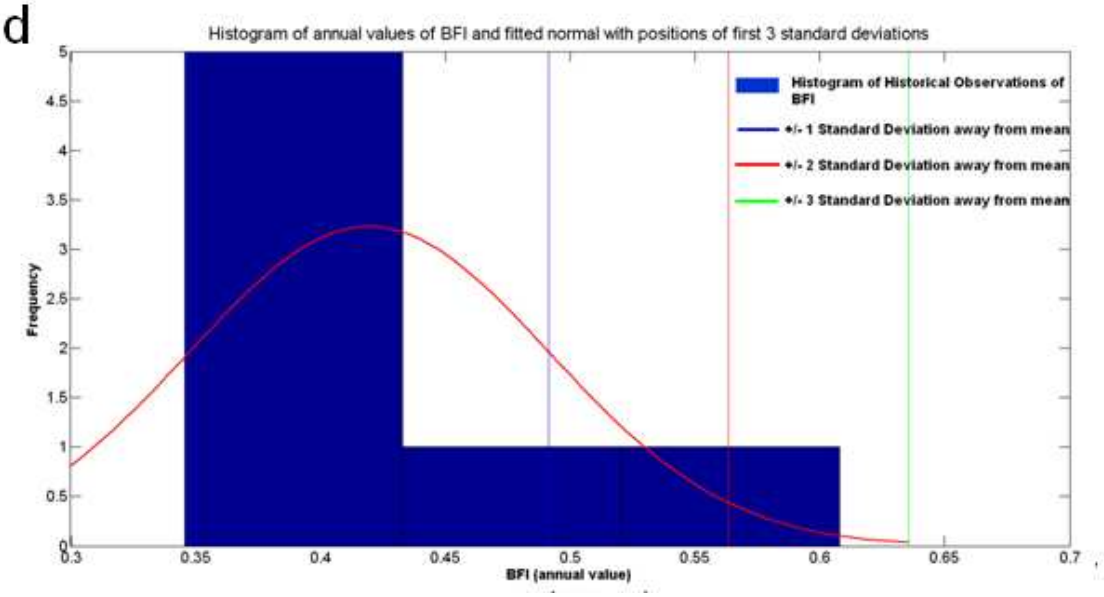
Histogram of annual values of BFI and fitted normal with positions of first 3 standard deviations
Histogram of Historical Observations of BFI
+/- 1 Standard Deviation away from mean
+/- 2 Standard Deviation away from mean
+/- 3 Standard Deviation away from mean
Frequency
BFI (annual value)

e

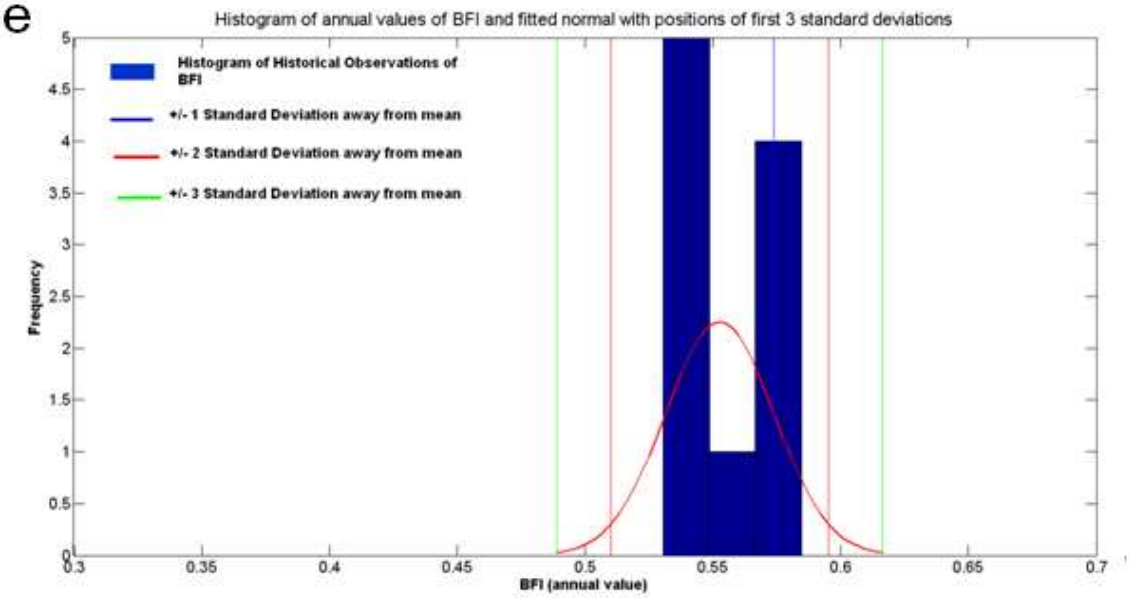
Histogram of annual values of BFI and fitted normal with positions of first 3 standard deviations
Histogram of Historical Observations of BFI
+/- 1 Standard Deviation away from mean
+/- 2 Standard Deviation away from mean
+/- 3 Standard Deviation away from mean
Frequency
BFI (annual value)

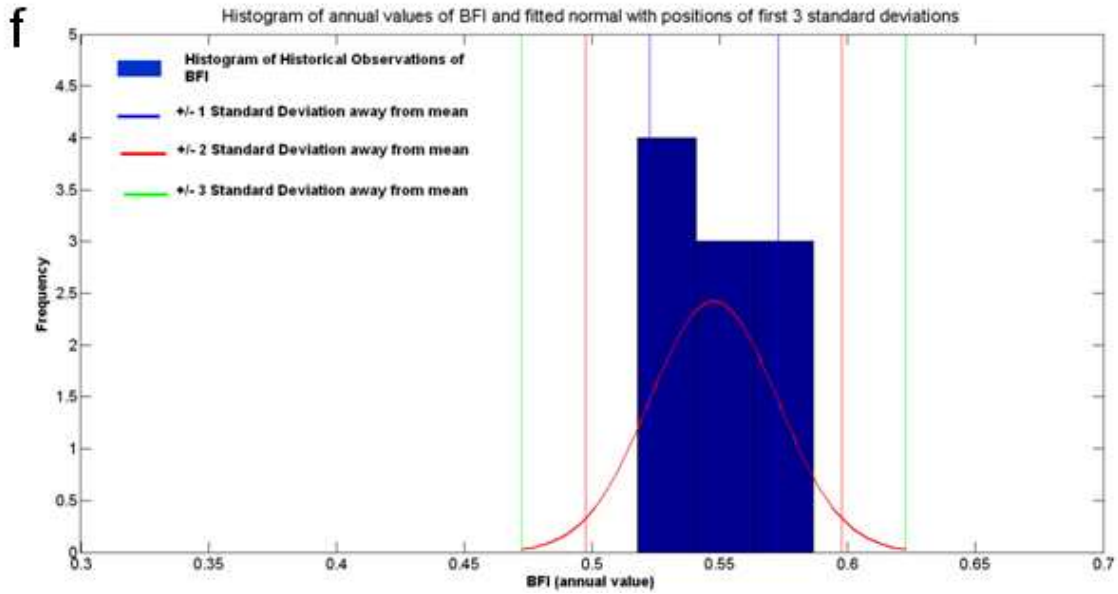

Figure D-1. Estimation of the range of base flow index to be used as constraints. The plots depict the histogram of base flow index calculated for each year for the period 1 October 1065 to 30 September 1975. The blue, red and green lines depict the ±1, ±2 and ±3 standard deviation limits. From the plot it is inferred that ±2 standard deviation covers the range of base flow index reasonably well. The watersheds are in order: (a) Lower Androscoggin, (b) Lochsa, (c) Escambia, (d) Meramec, (e) Peace and (f) Yampa.